PARALLEL SESSION ON BINARY AND LOW MULTIPLICITY REACTIONS

FINE STRUCTURE OF THE DIFFRACTION PEAK

V.A.Tsarev

P.N.Lebedev Physical Institute, Moscow, USSR

Recent measurements revealed rich structure of the differential cross section and polarization of the elastic hadron-hadron scattering. It is characterized by sequence of breaks, dips and bumps with typical intervals $\Delta t_\ell \gtrsim 1$ (GeV/c)^2 /1/. This ("large-scale") structure is usually assumed to be a manifestation of coherent effects originating from "hadron size" region $\lesssim 1$ Fermi.

The possibility of a small-scale structure with period Δt_s of order of 0.1 (GeV/c)^2 was also discussed theoretically/2,3/. Some experimental indication to this structure is perhaps present (?)/2/ in the ISR data/4/. New data presented at this Conference seem to give quite a clearcut evidence for such structure.

To begin with we show in Fig. 1 elastic proton-proton differential cross section measured at p=60 GeV/c at Serpukhov/5/. Experimental points are plotted with respect to commonly used smooth curve $(d\sigma/dt)_{AV} = A\exp(bt + ct^2)$ ("peak with break") and display distinct oscillations with period $\Delta t \sim 0{,}4$ (GeV/c)^2.

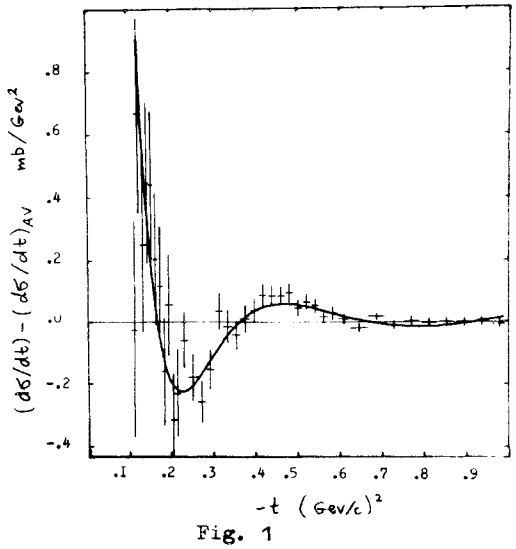

Fig. 1

The questions arise: What is the mechanism responsible for the small-scale oscillations (SSO)? Do they mean the existence of a new hadronic scale $\gg 1$ Fermi? We believe there is no need in any exotic dimensions. In fact SSO-phenomenon has been anticipated/2,3/ on the basis of ordinary scales ($t \sim 4\mu^2$ or $R \sim 1$ Fermi). It may arise simply due to edge effect caused by peripheral processes occurring mainly at impact parameters $\rho \sim 1$ Fermi.

It is instructive to consider an explicit model, but qualitative effect is not very sensitive to details and is model independent.

The main contribution to peripheral part $\Delta T(t)$ of elastic amplitude $T(t)$ is suggested in/3/ as coming from inelastic diffraction which is believed to have peripheral impact parameter profile/6/ (although there may be, of course, another contributions). Deck model with absorption/7/ was used to calculate the profile of diffractive dissociation contribution $\Delta G(\rho)$ into inelastic overlap function $G(\rho)$. Normalizing to diffractive cross section σ_D ($\simeq 6$ mb) the normalization parameter C has been fixed. The resulting profile (Fig. 2) is a "ring" with radius $R \sim \left\{2\ell \ln \frac{\sigma(B+B_1+\ell)}{4\pi\ell^2}\right\}^{1/2} \sim 0{,}9$ Fermi (Here $B \simeq \ell \simeq B_1 \simeq 10$ (GeV/c)$^{-2}$ are slopes of πN, NN scattering cross sections and π -meson vertex and propagator; $\sigma \equiv \sigma_{tot}(NN)$).

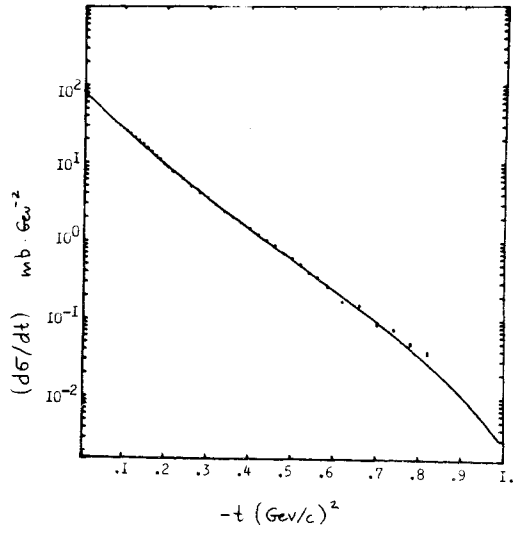

Fig. 2

Neglecting spin-flip and $\mathrm{Re}\ T$ contributions the S-channel unitarity gives $T(\rho) = 2i(1 - \sqrt{1 - G(\rho)})$, where $G = G_0 + \Delta G$, G_0 is a "central" term. Using the fact that $\Delta G(\rho)$ contributes mainly near $\rho \sim 1$ Fermi, where $G(\rho) \ll 1$, one can approximate elastic amplitude as $T(t) \simeq T_0(t) + \Delta T(t)$. $\Delta T(t)$ is the Fourier transform of $\Delta G(\rho)$ and exhibits expected Bessel - like behaviour*)

$$\Delta T(t) \sim i C \exp(at) J_0(R\sqrt{-t})$$

Inelastic diffraction is believed itself to give rise to absorption resulting in alternation of the ΔT sign. In other words the "central term" T_0 may be expected to have a simple form if one takes $T = T_0 - \Delta T$. Here $T_0(t)$ has a meaning of unabsorbed overlap fuction of true inelastic processes. So, we can consider both versions:

$$\frac{d\sigma}{dt} = \left\{ |T_0(t)|^2 \pm 2\, T_0^*(t)\, \Delta T(t) \right\} + |\Delta T(t)|^2 \quad (1)$$

First of all, it is easy to see that $|\Delta T(t)|^2$ gives rise to SSO (about "averaged" t-dependence) which are nicely confirmed by the data (see curve in Fig.1, $C = 4\ mb^{1/2}\mathrm{GeV}^{-1}$, $\alpha = 2{,}5\ (\mathrm{GeV/c})^{-2}$, $R = 5{,}0\ \mathrm{GeV}^{-1}$). Further, it is the absorptive (minus) sign which was shown by carefull analysis giving proper description of the "peak with break" with "simple" form for $T_0(t)$. Fig. 2 is an illustration with

$$T_0(t) = i C_1 \exp(a_1 t)\, J_1(R_1\sqrt{-t})/R_1\sqrt{-t}$$

corresponding to scattering off a disk with rounded edge ($C_1 = 26\, mb^{1/2}\mathrm{Gev}^{-1}$, $a_1 = 4.8\ \mathrm{Gev}^{-2}$, $R_1 = 4\ \mathrm{Gev}^{-1}$).

One can expect the "edge effect" to show up also at large $|t|$ leading to large - and small-scale structure due to $\Delta T(t)$ and $|\Delta T(t)|^2$. SSO have to manifest itself in other elastic reactions and at different energies. Indeed, one could probably find it in SLAC data[7] at 10 GeV/c and some $\pi^{\pm} p$ data at 4–6 GeV/c[8].

*) From t-channel point of view it can be described by complex singularities in j-plane /2,3/.

Another place to look for SSO is the high energy nuclear scattering. Here nuclear fragmentation plays the role of dissociation and characteristic scale is determined by nuclear radii. The verification of the SSO hypothesis[2,3] with nuclei has been done at JINR[9] in α-particle beam at p=17.9 GeV/c. The data are summarized in Fig.3 where difference of experimental and Glauber cross sections for $\alpha - C$, $\alpha - Al$ and $\alpha - Cu$ scattering is plotted. At small $|t|$ ($.007 < |t| < .1\ \mathrm{GeV}^2$) the data exhibit oscillatory structure (although it

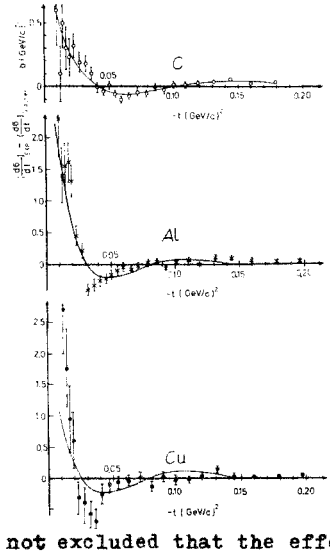

Fig. 3

is not excluded that the effect is introduced by inaccuratness of the Glauber description). Curves in Fig. 3 show the function $A_i J_0^2(R_i\sqrt{-t}) \exp(at) + c_i t + d_i$. The values of R_i found from the fit are of the order of radii of C, Al and Cu.

Detailed study of the nuclear fragmentation is of great interest in the light of present consideration.

We have discussed the model connecting the SSO with existence of peripheral inelastic diffraction. One can also try (especially for nuclei) to relate the SSO to fluctuations of the nuclear matter distribution ("shell effect"). However, as we know, the nuclear shell effects are expected to be shown up rather at large $|t|$ (small ρ) and have much larger period. Anyway one can hope to discriminate between these possibilities experimentally by comparing reactions

with and without diffractive dissociating probe (for instance, hadron-hadron and electron-hadron scattering).

In conclusion we want to emphasize that the SSO phenomenon giving interesting information on s- and t-channel aspects of high energy scattering has to be investigated further in great detail. The energy dependence is of particular interest. If $\sigma_{tot} \sim (\ell n s)^{\alpha}$ and elastic slope $B \sim (\ell n s)^{\beta}$ we expect

$$\Delta t^{-1} \sim R^2 \sim (\ell n s)^{\beta} [(\alpha-\beta)\ell n \ell n s + C].$$

The data available at present seem to confirm Δt decrease with s increasing.

I am grateful to A.M.Baldin, N.I.Starkov, L.N.Strunov and participants of E.L.Feinberg's seminar for useful discussions.

References

1. A.W.Hendry, Phys.Rev. D10, 2300 (1974). B.Schremp, F.Schremp, Phys.Lett. 55B, 303 (1975).
2. V.A.Tsarev, FNAL-Pub-74-17 (Jan. 1974).
3. N.I.Starkov, V.A.Tsarev, JETP Lett. 23, 403 (1976).
4. G.Barbellini et al., Phys.Lett. 39B, 663 (1972).
5. Y.M.Antipov et al. Paper No 40/A1-40 submitted to this Conference.
6. H.I.Miettinen, Proc. of the EPS Int.Conf. on High Energy Physics, Palermo, 1975.
7. V.A.Tsarev, Phys.Rev. D11, 1864, 1875 (1975).
8. R.K.Carnegie et al. Phys.Lett. 59B, 313 (1975).
9. G.Fox, C.Quigg, Compilation of Elastic Scattering data, UCRL-20001 (1970).
10. V.G.Ableev et al. Paper No 448/A6-5 submitted to this Conference and mini-rapport. talk by P.Zielinski at this Conference.

HIGH MASS DIFFRACTION EXCITATION OF PROTONS ON PROTONS AND DEUTRONS

S.V.Mukhin

Joint Institute for Nuclear Research, Dubna

In this short talk I shall discuss some new results of four papers, submitted to the Conference, on the inclusive processes

$$p + p \longrightarrow X + p$$

and

$$p + d \longrightarrow X + d$$

in the kinematic range $5 \leqslant M_x^2 \leqslant 0.25$ (GeV)^2, $S > 120$ GeV^2 and $t < 0.3$ (GeV/c)^2.

Two of them present the data obtained at Fermilab with deuterium (USSR-USA collaboration)[1] and hydrogen (C-SB collaboration)[2] jet targets. In these experiments the recoil particles from the interactions of an internal beam were detected by the solid-state detector telescopes.

The authors took special care for background corrections which were < 8% for the pd case and $\leqslant$ 2% for pp.

The two others from CERN-ISR present the single-arm spectrometer data obtained with deuteron (CHM-collaboration)[3] and proton (CHLM-collaboration)[4] circulating beams.

The high mass region is the region where the triple Regge phenomenology is expected to apply. Using the generalized optical theorem[5], the inclusive reaction a + b $\longrightarrow$ c + X can be related to three-body scattering amplitudes as shown in Fig. 1 and an invariant double differential cross section can be expressed as

$$S\frac{d^2\sigma}{dt\,dM_x^2}(S,t,M_x^2) = \frac{1}{S}\sum_{i,j,k} G_{i,j,k}(t)\left(\frac{S}{\nu}\right)^{\alpha_i(t)+\alpha_j(t)} \nu^{\alpha_k(0)},$$

where

$$\nu = M_x^2 - t - M_B^2.$$

The term $G_{i,j,k}$ denotes the triple Regge coupling of three Reggeons i, j and k, where the Regge poles i and j with trajectories

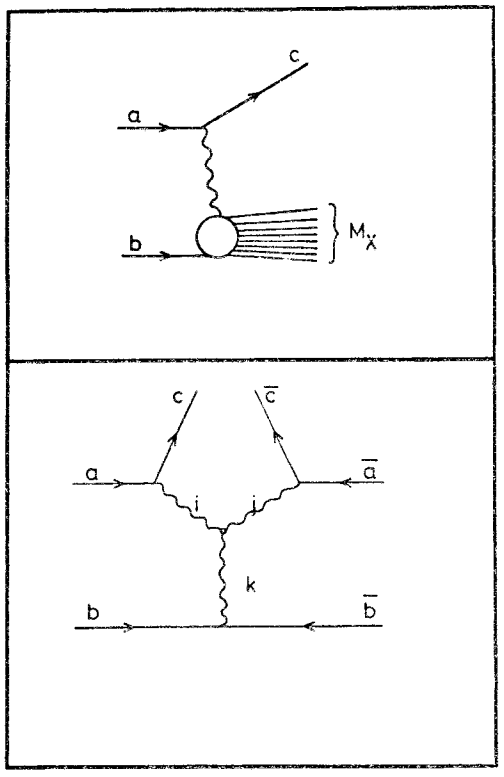

Fig. 1.
The quasi-two-body and associated triple Regge diagrams.

$\alpha_i(t)$, $\alpha_j(t)$, respectively, are exchanged and the Regge pole k with trajectory $\alpha_k(0)$ controls the Reggeon particle total cross section. Table 1 shows the corresponding coefficient of $G_{i,j,k}$ for $d^2\sigma/dt\,dM_x^2$ and $d^2\sigma/dt\,dx$, where $x \simeq p_{||}^{cm}/p_{max}^{cm} \simeq 1 - M_x^2/S$. One can see that the triple Regge terms have different M_x and S dependence and as diffraction (PPP, PPR), non-diffraction ($\pi\pi P$, $\pi\pi R$, RRP, PRR) and interference ones (RPR, RPP) have to dominate in different mass regions.

Since the London Conference it is well-known[6] that in the pure diffraction region $5 < M_x^2 < 0.05S\,GeV^2$ at small t-values the mass spectrum falls as $1/M_x^2$ with approximate scaling due to triple Pomeron (PPP) dominance whereas the fits of the data[7] show a significant role of the $\pi\pi P$ and $\pi\pi R$ terms as non-PPP background.

The comparison of the pp and pd data in the same kinematic range is at interest as the non-PPP background should be smaller in pd due to the isospin conservation.

Let us look at the new higher statistics data which cover a rather large M_x^2 region to better understand this phenomenon.

Figs. 2 and 3 show the USSR-USA collaboration pd inelastic mass spectrum at t =0.003

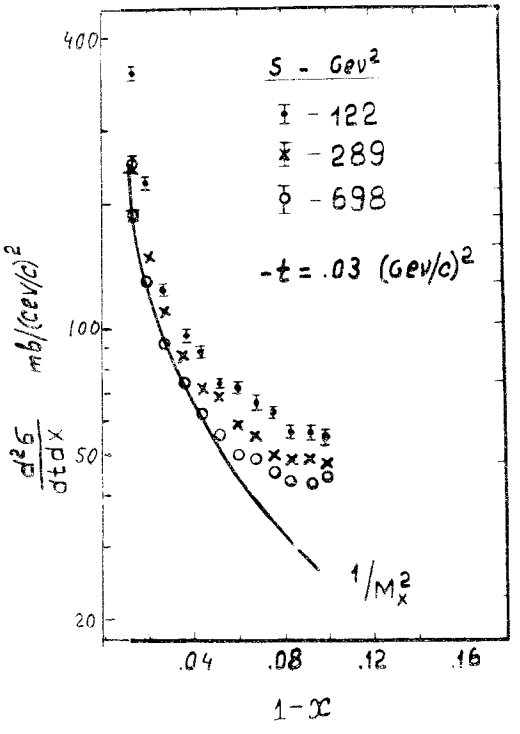

Fig. 2.
The invariant inelastic pd⟶Xd cross section divided by the deuteron coherence factor as a function of 1-X for S=122, 289 and 698 GeV^2 at t=0.03 (GeV/c)^2. The curve represents the behaviour adjusted to the high energy data.

and 0.13 (GeV/c)^2. The results are divided by the deuteron coherence factor $F_d(t) = (\sigma_t^{pd}/\sigma_t^{pp})^2 \times exp(-26.4|t| + 62.3t^2)$ in order to compare with the pp data. The energy dependence at $122 \leq S \leq 699$ GeV^2 is quite pronounced at these two values of t. The solid curves represent the $1/M_x^2$ behaviour fixed to be in agreement with the high energy points for $M_x^2/S < 0.05$.

There are clear deviations from this simple behaviour for $M_x^2/S > 0.06$.

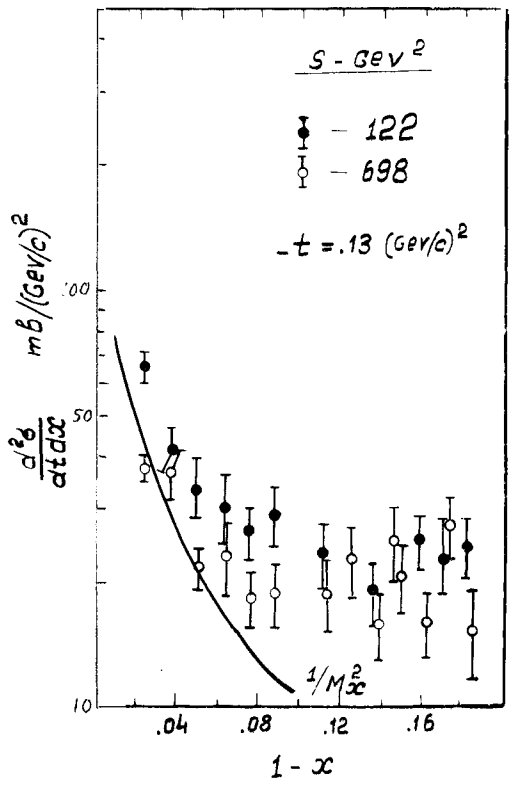

Fig. 3.
The invariant inelastic pd ⟶ Xd cross section divided by the deuteron coherence factor as a function of I-X for S=122 and 689 GeV^2 at t=0.13 (GeV/c)^2. The curve represents the $1/M_X^2$ behaviour adjusted to the high energy data.

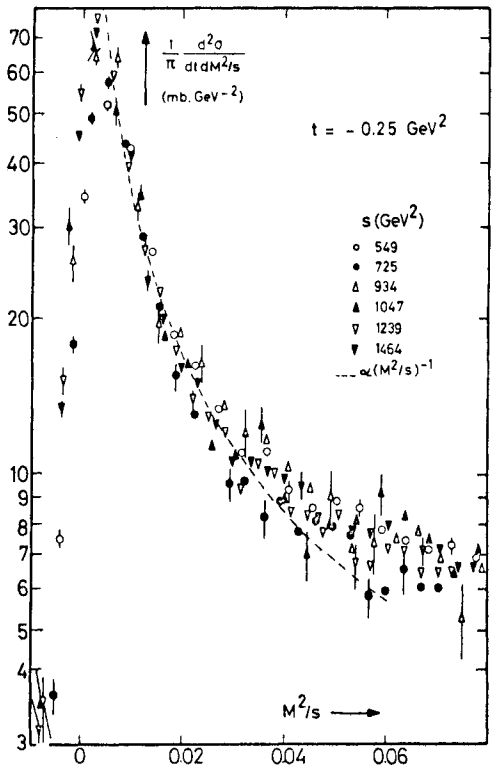

Fig. 4.
The invariant inelastic pp⟶Xp cross section at t=0.25 (GeV/c)^2 as a function of M_X^2/S and S. The dashed line shows the dependence of the form $(Mx^2/S)^{-1}$.

The new CERN ISR p-p data (CHLM collaboration) at $549 \leqslant S \leqslant 1464$ GeV^2 and t=0.25 (GeV/c)^2 in Fig. 4 also show the approximate $1/M_X^2$ mass spectrum dependence up to $M_X^2/S = 0.05$, but they scale well in terms of the variable M_X^2/S.

There arises a good question whether scaling occurs at $S > 600$ GeV^2 or at $t > 0.2$ (GeV/c)^2. Further experimental work is needed to get an answer to this question.

Returning to the region $M_X^2/S > 0.05$, where nondiffractive triple Regge terms have to be valid, I plot the pd (USSR-USA collaboration) and pp (C-SB collaboration) data at the same t values in Fig. 5. Distracting from normalization problems (both results are preliminary) and the difference in S, it is remarkable that the M_X^2 dependence is similar for the pp and pd processes.

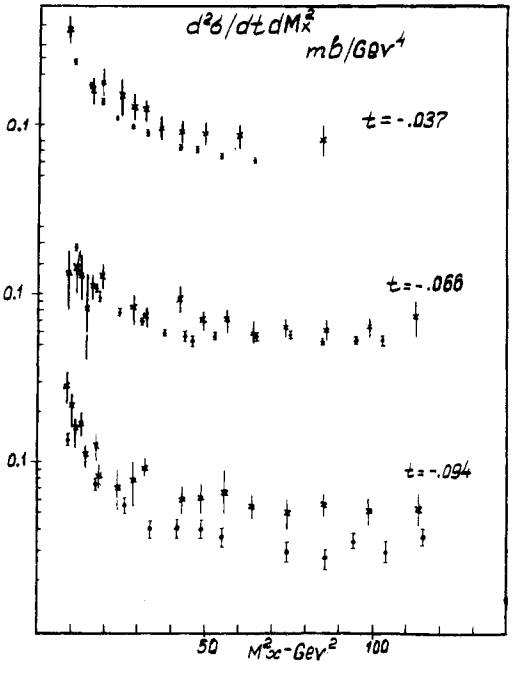

Fig. 5.
The M_X^2 dependence of $d^2\sigma/dt\,dM_X^2$ at fixed t=0.037, 0.068 and 0.094 (GeV/c)^2 for pp⟶Xp (x-points) at S≅940 GeV^2 and pd⟶Xd (o-points) at S=698 GeV^2.

In fig. 6 we can see CHM collaboration CERN-ISR results for the pp and pd inelastic spectrum at S=2800 GeV^2 and t=0.22 (GeV/c)^2.

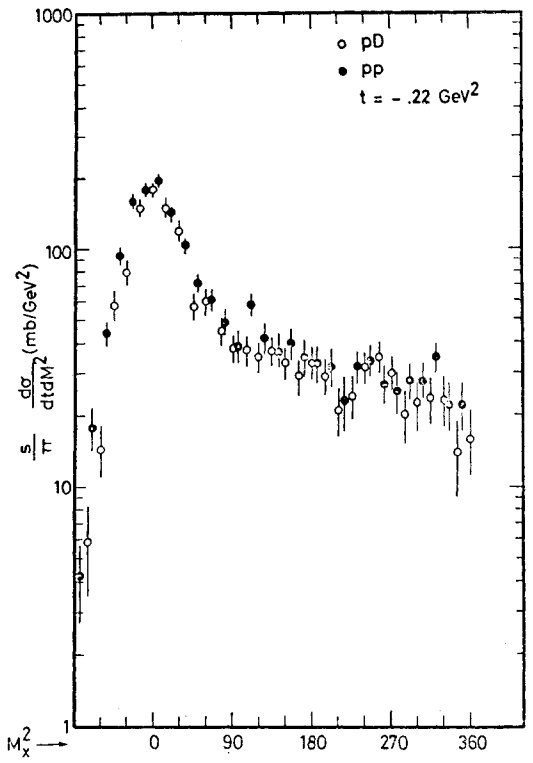

Fig. 6.
The invariant inelastic cross section versus M_x^2 for pp → pX (• -points) and pd→dX (o -points) at S=2800 GeV^2 and t=0.22 (GeV/c)^2. The pp cross section is scaled down by the ratio of the differential elastic cross section.

For comparison the pp → pX spectrum was scaled down by the measured ratio of the differential elastic cross sections for the two reactions. The striking feature of this graph in the resemblance between the pp and pd spectra over the whole M_x^2 range.

It seems there is good experimental evidence for a dominating role of the isospin =0 triple Regge components in exchange processes. In these four papers the authors do not report any deviations from the regular exponential t dependence like turn-overs, dips or breaks for inclusive inelastic pp and pd reactions.

The results of the discussion of the recent high mass inelastic data can be summarized as follows.

1. The triple Pomeron exchange dominates in the pure diffraction mass region $5 \leq M_x^2 \leq 0.055$ GeV^2.

2. There are deviations from scaling for $S \leq 600$ GeV^2 or $t < 0.2$ (GeV/c)^2.

3. The deviation from the $1/M_x^2$ behaviour for $M_x^2/S \gtrsim 0.06$ indicates a significant role of nondiffractive exchanges in this mass region.

4. The similarity at the pp and pd mass spectra shows that the isospin =0 exchange dominates.

5. There are no dips, breaks, turn-overs, etc.,in the t-dependence.

I should like to express my gratutude to S.Olsen and D.Gross who helped me in the preparation of this report.

Table 1.

Triple Regge Formulae, where
$\alpha_P(t) = 1.0 + \gamma t$, $\alpha_R(t) = \alpha_0 + \beta t$ and $\alpha_\pi(t) = 0.0 + \delta t$

Triple Regge Term	$d^2\sigma/dt\,dM_x^2$		$d^2\sigma/dt\,dx$	
i j k	Cosmic[a]	Full	Cosmic[a]	Full
P P P	$1/M_x^2$	$\frac{s^{2\gamma t}}{(M_x^2)^{1+2\gamma t}}$	$1/(1-x)$	$\frac{1}{(1-x)^{1+2\gamma t}}$
P R P	$1/(M_x^2\sqrt{s})$	$\frac{s^{\alpha_0+(\beta+\gamma)t-1}}{(M_x^2)^{\alpha_0+(\beta+\gamma)t}}$	$1/(1-x)^{1/2}$	$\frac{1}{(1-x)^{\alpha_0+(\beta+\gamma)t}}$
R R P	$1/s$	$\frac{s^{2\alpha_0+2\beta t-2}}{(M_x^2)^{2\alpha_0+2\beta t-1}}$	1	$\frac{1}{(1-x)^{2\alpha_0+2\beta t-1}}$
P P R	$1/M_x^3$	$\frac{s^{2\gamma t}}{(M_x^2)^{2-\alpha_0+2\gamma t}}$	$\frac{1}{\sqrt{s}(1-x)^{3/2}}$	$\frac{(M_x^2)^{\alpha_0-1/2}}{\sqrt{s}(1-x)^{3/2+2\gamma t}}$
P R R	$1/(M_x^2\sqrt{s})$	$\frac{s^{\alpha_0+(\beta+\gamma)t-1}}{(M_x^2)^{1+(\beta+\gamma)t}}$	$\frac{1}{\sqrt{s}(1-x)}$	$\frac{1}{s^{1-\alpha_0}(1-x)^{1+(\beta+\gamma)t}}$
R R R	$1/(sM_x)$	$\frac{s^{2\alpha_0+2\beta t-2}}{(M_x^2)^{\alpha_0+2\beta t}}$	$\frac{1}{\sqrt{s(1-x)}}$	$\frac{1}{s^{1-\alpha_0}(1-x)^{\alpha_0+2\beta t}}$
$\pi\pi P$	M_x^2/s^2	$\frac{s^{2\delta t-2}}{(M_x^2)^{2\delta t-1}}$	$(1-x)$	$\frac{1}{(1-x)^{2\delta t-1}}$
$\pi\pi R$	M_x/s^2	$\frac{s^{2\delta t-2}}{(M_x^2)^{2\delta t-\alpha_0}}$	$\sqrt{\frac{(1-x)}{s}}$	$\frac{1}{\sqrt{s}(1-x)^{2\delta t-\alpha_0}}$

a) Cosmic is defined by $\gamma = \beta = \delta = 0, \alpha_0 = 1/2$

References

1. Y.Akimov et al., Dubna-Fermilab-Rockefeller--Rochester-Arisona (USSR-USA) Collaboration, Proton Excitation to High Mass States on Deuterium, paper No 1262 (A1-171) submitted to this Conference.
2. S.Childress et al., Columbia-Stony Brook Collaboration, Proton-Proton Inelastic Scattering at 0.5 TeV, paper No 829 (A1-169) submitted to this Conference.
3. J.C.M.Armitage et al., CERN-Holland-Manchester Collaboration, High Mass Single Diffraction Excitation in dp $\longrightarrow$ dX at S=2800 GeV^2, paper No 345(A1-170)submitted to this Conference.
4. M.G.Albrow et al., CERN-Holland-Landcaster-Manchester Collaboration, Inelastic Diffraction Scattering at the CERN ISR, paper No 799 (A1-90) submitted to this Conference.
5. A.H.Müller, Phys.Rev., D2, 2963 (1970).
6. See, for instance, Y.Akimov et al., Proton-Deuteron Elastic Scattering and Diffraction Dissociation from 50 to 400 GeV, Rockefeller Univ. preprint COO-2232A-I and contribution to the XVII Intern.Conf. on High Energy Physics, London (1974).
7. R.D.Field, E.C.Fox. Nucl.Phys., B80, 367 (1974).

NUCLEON DIFFRACTION DISSOCIATION (EXPERIMENT)

Yu.Kamyshkov
ITEP, Moscow, USSR

In this paper the present situation in nucleonic diffraction dissociation into $(N\pi)$-system is discussed. New experimental data have come mainly from experiments performed at high energies by electronics technique [1-4] at Serpukhov, FNAL and ISR with high statistics.

The main features of nucleon diffraction dissociation $N \to N\pi$ observed at intermediate energies (< 30 GeV) are the following. The $(N\pi)^-$ system is preferably produced with low invariant mass. The energy dependence of the reaction is rather weak. The t-distribution shows diffraction - like behaviour ($\sim e^{Bt}$) with the slope B, which depends on the mass of the $(N\pi)^-$ -system. For the nucleon of the system, the $\cos\theta_{GJ}$ distribution is strongly peaked towards $\cos\theta_{GJ}=+1$. Azimuthal φ_s and φ_t distributions are not uniform and hence are not in agreement with S- and t-channel helicity conservation.

1. Manifestation of Baryon-exchange Deck-effect

Fig. 1 shows the angular distribution over $\cos\theta_{GJ}$ as obtained by Moscow-Karlsruhe-CERN Collaboration[1] in all experimental phase space (a) and under small M and $|t|$ restrictions (b). One can be sure that the influence of resonance production is considerably weakened by this restrictions.

Forward peak near $\cos\theta_{GJ} \sim +1$ can be described as π -exchange Deck-effect (dotted). But quite pronounced backward peak near $\cos\theta_{GJ} \sim -1$ is not consistent with π -exchange. This backward peak can be explained by a mechanism which is similar to the Deck one, but involving baryon exchanges instead of pion exchange[9] (solid).

In fig. 2, one can see that taking into account baryon-exchange Deck graphs' contributions

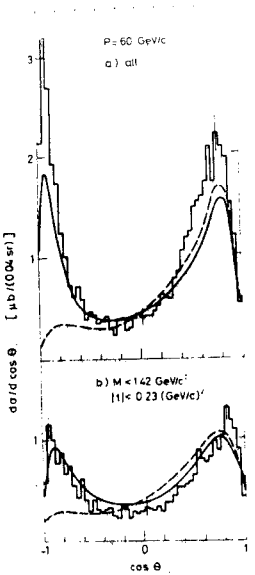

Fig. 1

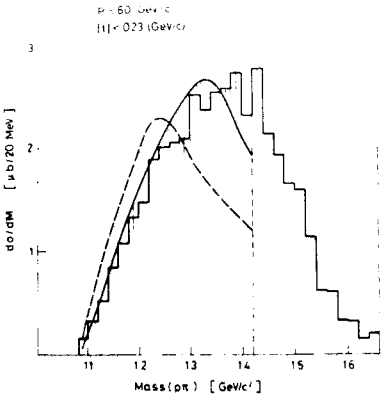

Fig. 2

improves mass spectrum description considerably (π -exchange Deck alone predicts too soft mass spectrum).

The backward peak near cos $\theta_{GJ} \sim -1$ at small M and $|t|$ was also clearly seen in FNAL[2] and ISR[3] experiments. Authors of[2] compared φ_{GJ} -distributions at cos $\theta_{GJ} \sim +1$ and cos $\theta_{GJ} \sim -1$ with reggeized Deck model predictions (fig. 3). They consider the φ_{GJ}-distribution structure to be a manifestation of baryon-exchange Deck-effect.

So we have now at least three arguments for the existence of baryon-exchange Deck mechanism, i.e., backward peak at cos $\theta_{GJ} \sim -1$, mass spectra discription and φ_{GJ} structure.

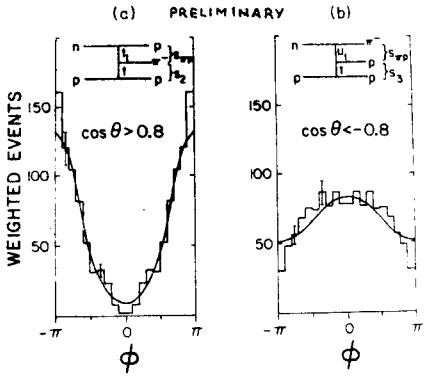

Fig. 3

2. t-distributions. Correlations

The appearence of the structure in $d\sigma/dt$ near $|t| \sim 0.2$ (GeV/c)^2 in DD-processes was recently discussed[2,3,9]. The new data have come from CHOV experiment[3] at ISR the deep in t-distributions has been observed. Fig. 4 (b) shows that for the mass range 1.30-1.35 GeV the deep is most pronounced for the cos $\theta_{GJ} \sim 0$. Fig. 4 (a) presents the t-distributions for $-0.3 < \cos\theta_{GJ} < 0.3$ at different mass intervals. The deep is clearly seen for the masses M < 1.4 GeV and moves to higher $|t|$ values with mass increasing.

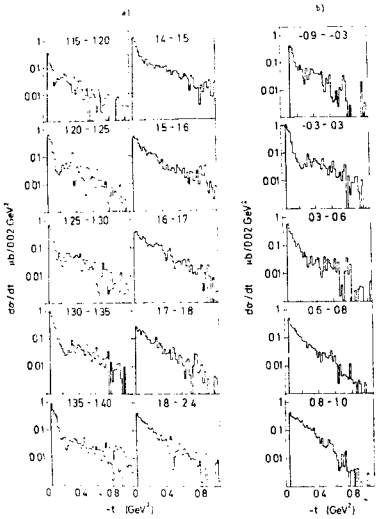

Fig.4

Deck-type model with absorption, perhaps, can interpret the appearence of this structure /9 and ref. therein/.

Collection of the data on mass-slope correlation is shown in fig. 5. One can see that in the momentum range 12-1000 GeV/c the shape of

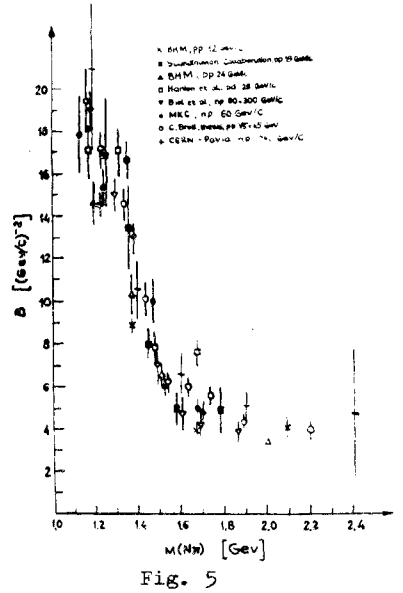

Fig. 5

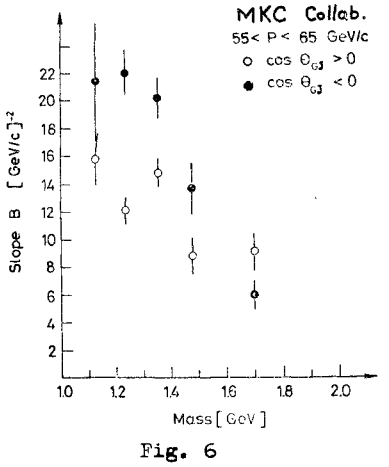

Fig. 6

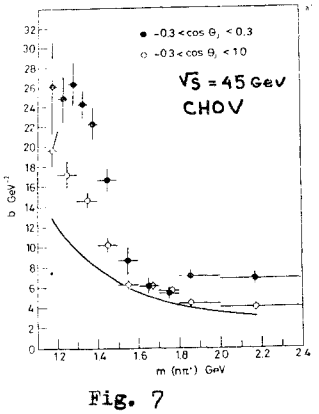

Fig. 7

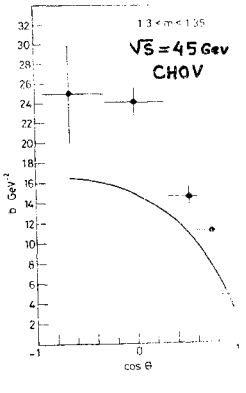

Fig. 8

the function is universal; at small masses the slope is about twice that of NN elastic one and for M≥1.6 GeV is about a factor of 2 less.At small masses(<1.3 GeV)there are some indications to increasing of the slope with the energy,but due to large experimental errors one can hardly say that the energy dependence of the slope inall mass intervals is different from that of elastic scattering. New experimental results[1,2,3] show the existence of the correlation between production and decay of $(N\pi^-)$ system (fig. 6-8). Theoretical description of the slopes is discussed in[9]. At least partially these correlations can be explained kinematically.

3. Mass spectra and cross sections

In fig. 9 the $(p\pi^-)$ mass distribution for $45 \leq p_n \leq 65$ GeV/c[1] is compared with the corresponding preliminary distribution from the FNAL experiment[2]. Both sets of data are absolutely normalized. The spectra turned out to be almost identical, apart from the mass region around 1.5 GeV.

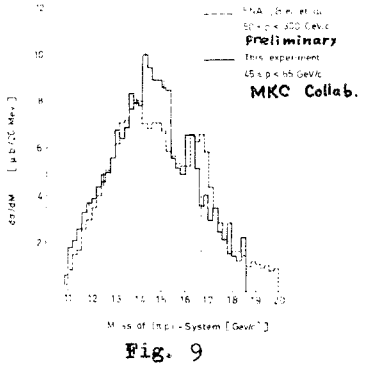

Fig. 9

Fig. 10 shows energy dependence of the cross sections integrated over two low mass intervals for $0.002 < |t| < 1.0$ (GeV/c)^2[1,2,7]. One can see that in the error bars low mass cross sections are energy independent.

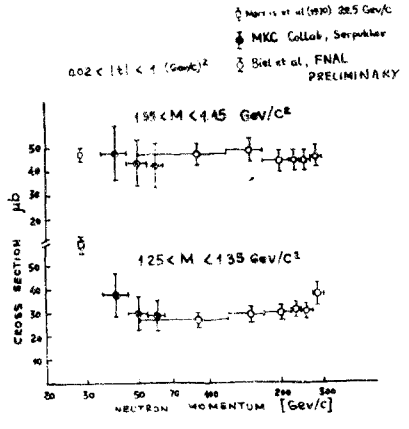

Fig. 10

Mass spectra for Serpukhov and ISR experiments

are presented in fig. 11 under the same phase space distributions. All masses with the exception of the interval near $M \sim 1.5$ Gev display equal cross sections.

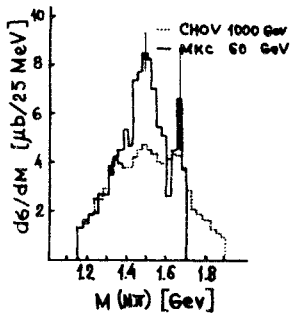

Fig. 11

If high energy diffraction dissociation is dominated by isospin $I = 0$ exhange, cross section for the reactions $pp \to (n\pi^+)p$ and $np \to (p\pi^-)p$ should be equal (total DD pp cross sections have a trivial factor 2). Fig. 12 shows experimental data on total nucleon dissociation cross section in the momentum range from 7 to 1500 GeV/c[1-7]. At ISR energies np and pp channels have equal cross sections within the experimental errors. At the energies above Seprukhov range cross sections seem to be flattened.

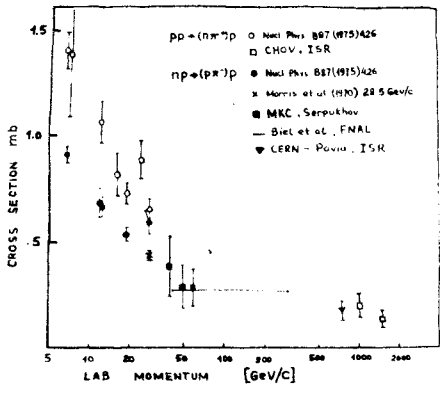

Fig. 12

I wish to thank Prof. V.A.Lyubimov and Dr. L.A.Ponomarev for useful discussions and some essential remarks.

References

1. A.Babaev et al., Paper 29/A1-29.
2. J. Biel et al., Papers 909/A1-8,69/A1-69. T.Ferbel, UR-541 (The University of Rochester, New York 1975). The latest contribution to the Conference contains more detailed analysis of differential cross sections in approximately whole phase space. Data are based on 80000 events.
3. H. de Kerret et al., Paper 65/A1-65. C.Broll, Thesis, Orsay, 1976.
4. CERN-Pavia Collab. Paper 338/A1-102.
5. E.Dahl-Jensen et al., Nuclear Phys., B87, 426 (1975).
6. V.Bakken et al., Paper 74/A1-74.
7. T.W.Morris et al., Comparison of Reactions $pp \to pn\pi^+$ and $pn \to pp\pi^-$ in pp and pd Interactions at 28.5 GeV/c. Paper submitted to the 15-th Int. Conf. on High Energy Phys., Kiev, 1970.
8. D.Denegri et al., Paper 73/A1-75.
9. L.A.Ponomarev. Mini-rapporteur's talk at this Conference.

SPIN DEPENDENCE STUDIES WITH THE ZGS POLARIZED PROTON BEAM

A.B.Wicklund

A.N.L., U S A

We summarize here selected results from recent measurements using the polarized proton beam at the Argonne Z.G.S.

1. Elastic $p_\uparrow p_\uparrow \to pp$ at large $p_\perp$:

Using polarized proton beam and target, the Michigan-A.N.L.-St.Louis collaboration[1] has measured both the polarized target asymmetry A, and the beam-target spin correlation C_{NN} at 6 and 12 GeV/c (Fig.1). What is remarkable

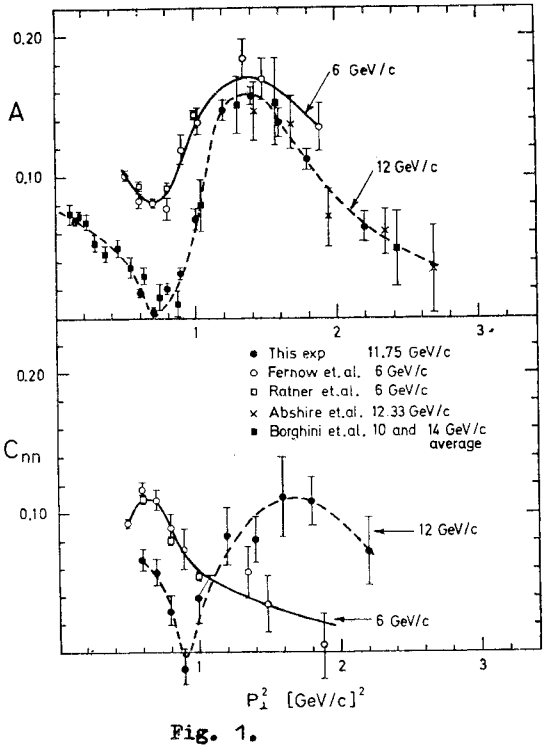

Fig. 1.
The parameters A and C_{NN} measured in $p_\uparrow p_\uparrow \to pp$ at 6 and 12 GeV/c.

is that in the secondary maximum region of $p_\perp^2$ (1 to 2 GeV^2), A is slowly varying with energy while C_{NN} increases considerably going from 6 to 12 GeV/c. Furthermore, C_{NN} develops a sharp dip structure at 12 GeV/c which is not seen at the lower energies. An obvious interpretation is that the spin dependent part of the pp elastic amplitude falls more slowly with energy than the nonflip diffractive component at large $p_\perp^2$. This behaviour is not anticipated by conventional models.

II. Comparison of elastic $p_\uparrow p \to pp$ and $p_\uparrow n \to pn$ polarizations

The effective mass spectrometer (E.M.S) has been used to measure pn elastic asymmetries for the first time above cyclotron energies[2]. From 2 to 6 GeV/c (Fig.2) the pn polarization falls faster with energy than the pp.

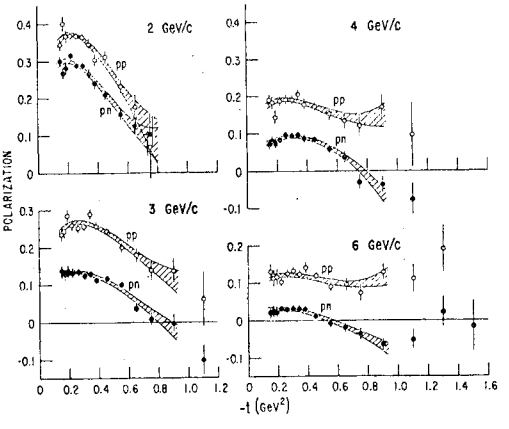

Fig. 2.
The polarization parameters in pp and pn elastic scattering at 2,3,4, and 6 GeV/c.

Since the polarization is given by natural mines-parity exchanges (e.g. ρ, ω, B and A_2 exchange flip amplitudes interfering with the Pomeron), Regge models expect that pp and pn polarizations should seal in the same way with energy. The data shows that the pp and pn polarization tend to approach mirror symmetry as the energy increases, implying that the I=1 exchange flip amplitude falls more slowly with energy then the I=0 term. In fact, the effective Regge trajectory of the I=0 exchange flip amplitude is empirically one unit lower than conventional ω and B trajectories, and the data can be satisfactorily fitted only by introducing ad hoc low-lying trajectories that are not anticipated from meson-baryon reactions.

III. Charge exchange production of N^* and Δ^{++}.

The E.M.S. has been used to study the reactions[3]

$$p_\uparrow p \to p\pi^+ n \text{ (2000000 events)} \quad (1)$$

$$p_\uparrow n \to p\pi^- p \text{ (150000 events)} \quad (2)$$

from 2 to 6 GeV/c. For small $-t$ ($-t < 0.2$ GeV^2) these reactions should be dominated by π exchange and the spin-dependence effects can be compared with polarizations measured (in $\pi^- p$ elastic scattering). Fig.3 shows the small -t cross sections for reactions (1) and (2) versus $p\pi^+$

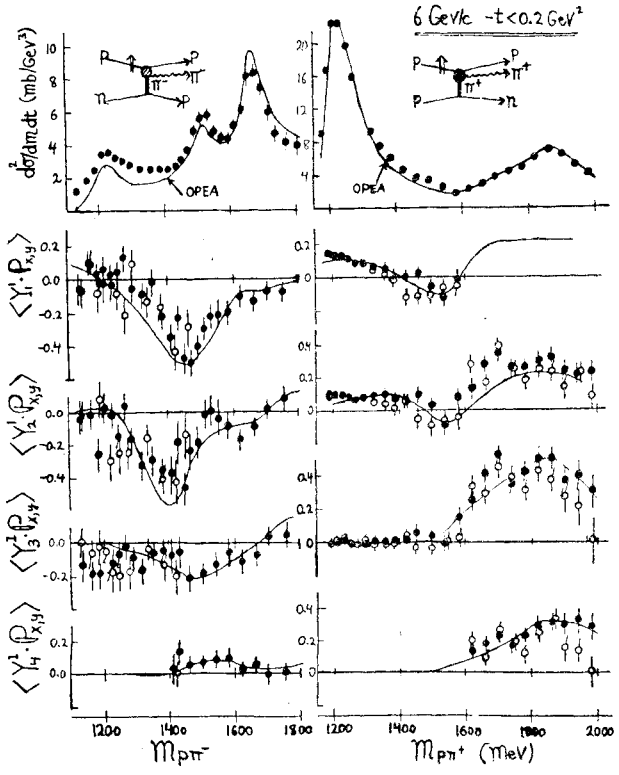

Fig.3.

Cross sections and polarizations versus $p\pi^-$ and $p\pi^+$ masses for reactions $p_\uparrow n \to p\pi^- p$ and $p_\uparrow p \to p\pi^+ n$. The solid points are correlations $\langle I_m Y_L^1 \cdot P_x \rangle$; the open points are $\langle Re\, Y_L^1 \cdot P_y \rangle$, where P_x (P_y) are transverse polarization components in the scattering plane (normal to the scattering plane).

and $p\pi^-$ masses; the correlations of the spin vector with the decay moments Y_L^1 are also shown and compared with absorbed π-exchange calculated with measured elastic phase shifts. Agreement with OPEA is reasonably good.

At larger -t values other mechanisms besides π-exchange become important. Fig. 4 shows unpolarized density matrix elements in the S channel for $p_\uparrow p \to \Delta^{++} n$ at 6 GeV/c. Considerable structure can be seen. The polarized beam asymmetries at 3,4 and 6 GeV/c are also shown; these are substantial (40% for $\sqrt{-t} > 0.5$ GeV/c) and show little if any variation with energy. These asymmetries would arise in Regge models from π-B or ρ-A_2 exchange interference, and would vanish if the exctic $pp \to \Delta n$ amplitudes were purely real.

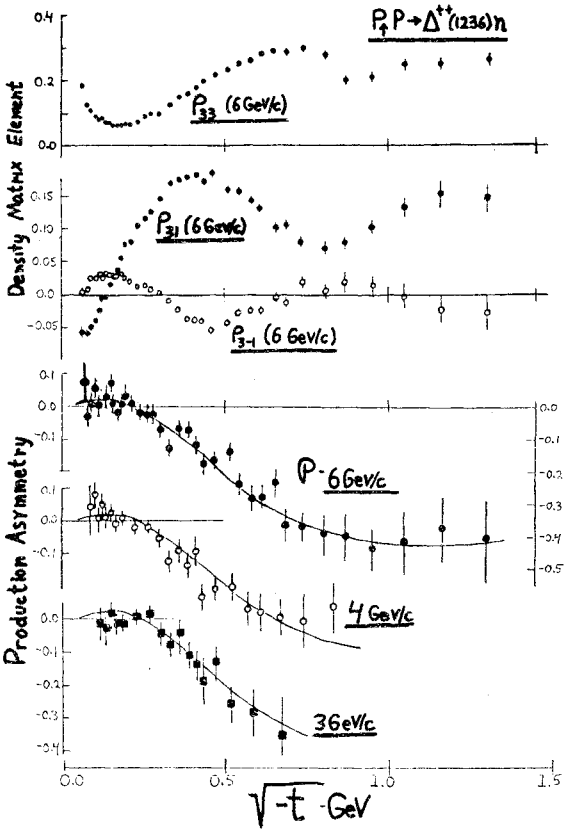

Fig.4.

Density matrix elements at 6 GeV/c and overall polarization asymmetry at 3,4 and 6 GeV/c for $p_\uparrow p \to \Delta^{++} n$.

IV. Inelastic diffraction at 6 GeV/c

The 3-body diffraction dissociation reactions have been measured at 6 GeV/c with hydrogen and deuterium targets[3]:

$$p_\uparrow p \to p\pi^+\pi^-(p) \text{ (500000 events)}, \quad (3)$$

$$p_\uparrow d \to p\pi^+\pi^-(p_{sp}) \text{ (250000 events)}. \quad (4)$$

The uncorrected mass spectra are shown in Fig.5 for two different $p_\perp^2$ regions. For $p_\perp^2 < 0.02$ GeV^2 peaks are seen at 1425 and 1660 MeV $p\pi^+\pi^-$ mass.

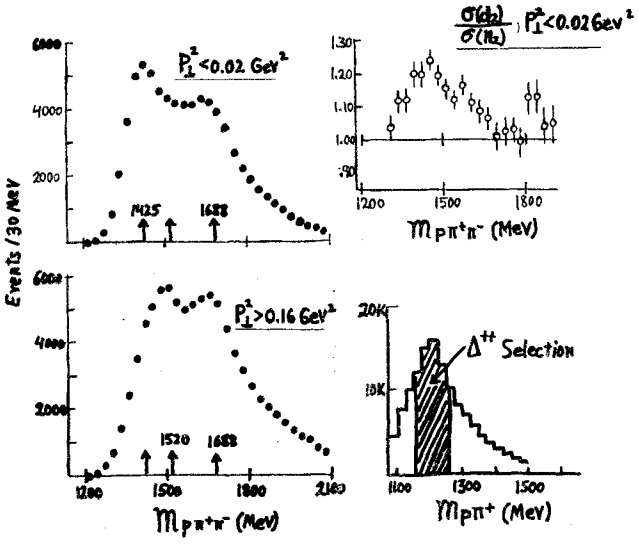

Fig. 5.
$p\pi^+\pi^-$ mass spectra from $p_\perp p \to p\pi^+\pi^- p$ for $p_\perp^2 < 0.02$ and $p_\perp^2 > 0.16$ GeV^2.

For $p_\perp^2 > 0.16$ GeV^2, the low mass peak migrates to 1500 MeV. Comparison of hydrogen and deuterium cross sections for $p_\perp^2 < 0.02$ GeV^2 reveals a considerable coherent contribution off deuterium, which has a $\sim$20% larger cross section per nucleon than hydrogen.

As in the case of π-exchange reactions discussed above, polarization effects can arise in the $\Delta^{++}\pi^-$ system from interference of partial waves having different production or decay phases. In particular, diffractive resonance production (90° production +90° decay phase) can interfere with the large S wave $\Delta\pi$ Deck amplitude (90° production). Since the dominant Deck S wave is $J^P = 3/2$, the only known resonant states that can produce polarization are the $J^P = 1/2^+$ and $J^P = 5/2^\pm$ states (the $3/2^-$ N*(1520) has the same J^P as the Deck amplitude and can therefore not produce polarization). The main signature of the $1/2^+$ Roper resonance is that only helicity -1/2 Δ^{++}, S can be produced in the decay N*(1470) $\to \Delta\pi$. Selecting $p_\perp^2 < 0.12$ GeV^2, the production mechanisms should be simple (i.e. helecity conserving), and should not affect the polarization asymmetries.

The asymmetry is defined as the correlation between the proton spin vector and the $N^* \to \Delta\pi$ decay normal. Fig. 6 shows the asymmetries for helicity 1/2 and 3/2 Δ states for different $\Delta\pi$ mass intervals, plotted against the $N^* \to \Delta\pi$ decay cosine. Large asymmetries are seen for masses below 1600 MeV in the helicity 1/2 state only; the asymmetry in helicity 3/2 Δ production is large only for masses above 1600 MeV where $5/2^\pm$ resonances are important. The fact that the asymmetries are confined to helicity -1/2 Δ states suggests that the dominant interference effect is between the $1/2^+$ Roper resonance and the $3/2^-$ S-wave Deck background. The fitted curves in Fig.6 assume a constant 90° phase difference between these two waves, roughly consistent with the known slow variation with mass of the $1/2^+$ state. The measured asymmetry is consistent with a very small $1/2^+$ cross section ($\sim$5% of Deck) and a +90° phase for the $1/2^+$ production amplitude.

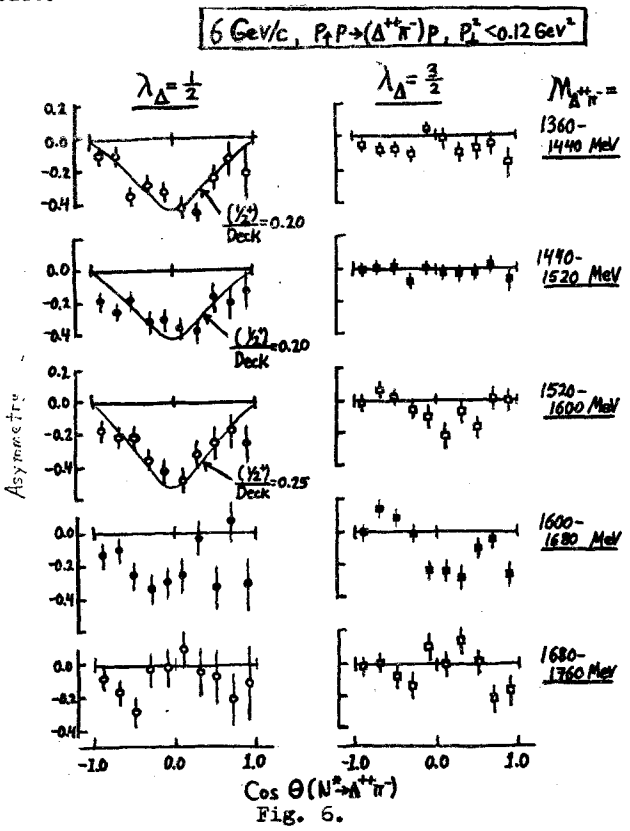

Fig. 6.
Polarization asymmetry for helicity 1/2 and 3/2 Δ states in 5 $\Delta\pi$ mass intervals, plotted against the Gottfried-Jackson $\Delta\pi$ decay cosine.

References

1. K.Abe et al., **Measurement of Proton-Proton Elastic Scattering in Pure Initial Spin States at 11.75 Gev/c (Univ. of Mich. preprint submitted to this conference) 1209/A1-162.**
2. R.Diebold et al., **Measurement of the Proton-Neutron Elastic Scattering Polarization from 2 to 6 GeV/c, paper 1153/A1-153.**
3. A.B.Wicklund et al., **Study of Inelastic Reactions with a Polarized Proton Beam, paper 61/A1-61.**

BARYON EXCHANGE IN 12 GeV/c $\bar{n}p$ INTERACTIONS

M.W.Arenton, W.J.Bacino, J.M.Hauptman, C.F.May, F.D.Rudnick, W.E.Slater, D.H.Stork, H.K.Ticho

University of California, Los Angeles

P.F.Shepard

University of Pittsburgh

R.A.Gearhart

Stanford Linear Accelerator Center

(present by D.H.Stork)

We report preliminary results on the production of boson states B° by baryon exchange in reactions of the type $\bar{n}p \to nB^{\circ}$ at an incident momentum of 12 GeV/c. Baryon exchange has been extensively studied in elastic scattering and charge exchange reactions. However, data on inelastic reactions at energies as high as 12 GeV/c are rare[1,2].

We have carried out this experiment by photographing the SLAC 40" hydrogen bubble chamber operating in its rapid cycling mode on detection of the energetic forward neutron. The trigger apparatus was 5 meters downstream of the chamber. The beam, bent by the bubble chamber magnet, just missed the apparatus.

The first element in the apparatus is an anticounter package of two 1.25 cm. sheets of lead and 2 scintillators to veto charged particles and photons. The remainder of the apparatus is a calorimeter. Interspersed in the front part of the calorimeter are eleven optical spark chambers. By measuring the vertex point of the hadronic shower made by the neutron as well as its production vertex in the bubble chamber the direction of the neutron is established. Events with no other neutral secondaries besides the neutron yield three constraint fits.

The calorimeter is 79 x 79 cm^2 in cross section and has 26 modules. The first 11 of these contain four gap spark chambers with lead plates. Each calorimeter had its own phototube

and a sum pulse from the calorimeter was formed electronically.

The trigger for the experiment was the simple requirement of no count in the anti-counters and a sum pulse greater than a calibrated threshold in the calorimeter. Typical running conditions were 10 expansions per second and 6 pions per pulse. The trigger rate was about 180 per hour. A total of 242,500 triggers were taken. This required 6.5×10^7 expansions of the 40" chamber.

The film was scanned for all event types. About 35,000 2-prong and 30,000 4-prong events were measured on the UCLA measuring system, MOLLY. The neutron interaction vertex in the spark chambers was reconstructed in space with standard deviation of 1.25 cm in transverse position. The measurements were processes through TVGP and SQUAW.

There are a number of corrections to the data. We assign a weight to each event equal to the inverse probability that it caused a trigger. The most important part of this weight is the triggering probability as a function of neutron momentum. We have made a cut excluding events with neutron momentum less than 7 GeV/c. This avoids events whose weight is greater than 5 and eliminates events with recoil mass ≥ 3.1 GeV.

The most fully analyzed data concern the reaction $\pi^- p \to n \pi^- \pi^+$ and we shall concentrate on it. There are 344 samples of this reaction. None of these events are ambiguous with other three constraint hypotheses. The contamination due to reactions with additional missing neutrals is estimated to be at most 10% and is flat in $\pi^- \pi^+$ mass.

Figure 1 shows the mass distribution of the $\pi^- \pi^+$ system. The mass resolution is always substantially smaller than the width of the bins. Peaks at the ρ and f masses are evident. No other structure is evident. Events that appear as a Δ^- peak in the $\pi^- n$ mass plot are shown

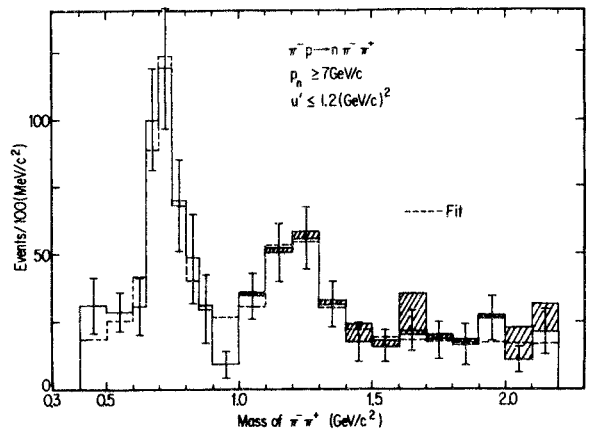

Fig. 1

cross hatched. These Δ^- events were not included in the fit to the mass distributions which was made with Breit-Wigner shapes having energy dependent widths for the ρ and f plus a constant background term.

The bin from .9 to 1.0 GeV/c^2, with only a few events, has an undue influence on the fitting procedure and was rejected. The best fit is shown in Figure 1. It has $\chi^2 = 8.0$ for 13 degrees of freedom.

The parameters of the best fit are $M_\rho = 0.716 \pm 0.007$ GeV, $\Gamma_\rho = 0.128 \pm 0.025$ GeV, $M_f = 1.204 \pm 0.017$ GeV, $\Gamma_f = 0.187 \pm 0.068$ GeV. According to the fit, the data consists of 171 ± 21 ρ's, 118 ± 27 f's and 16.5 ± 2.0 background events per 100 MeV. The widths of the ρ and f are in good agreement with the accepted values. The masses are both lower than the accepted values. This may results from low statistics and an unrealistic background treatment, but it is interesting to speculate that this may be a dynamical effect, particularly since an experiment at 6 GeV/c also finds a low ρ mass[13].

The total cross sections for $0 < u < 1.2$ (GeV/c)^2, where $u' = u_{max} - u$ are 0.61 ± 0.11 μb for ρ's and 0.49 ± 0.13 μb for f's.

The differential cross sections $d\sigma/du'$ for ρ's and f's are shown in Figure 2. We define the ρ mass range to be $0.62 \leq m_\rho \leq 0.90$ GeV and the f mass range $0.90 \leq m_f \leq 1.43$ GeV. No specific background subtraction was made in determining

the differential cross sections since the events outside of the resonant regions show similar U' dependence. However, the absolute scales of the $d\sigma/du'$ plots have been normalized to give the total cross section obtained from fitting the mass plot. The $d\sigma/du'$ distributions are consistent with simple exponentials. Least squares fits to the form $Ae^{xp}(-Bu')$ give $A=1.3\pm0.2$ μb $(GeV/c)^2$, $B=2.0\pm0.4$ $(GeV/c)^{-2}$ for ρ's and $A=1.0\pm0.3$ μb $(Gev/c)^2$, $B=1.9\pm0.4$ $(GeV/c)^{-2}$ for f's.

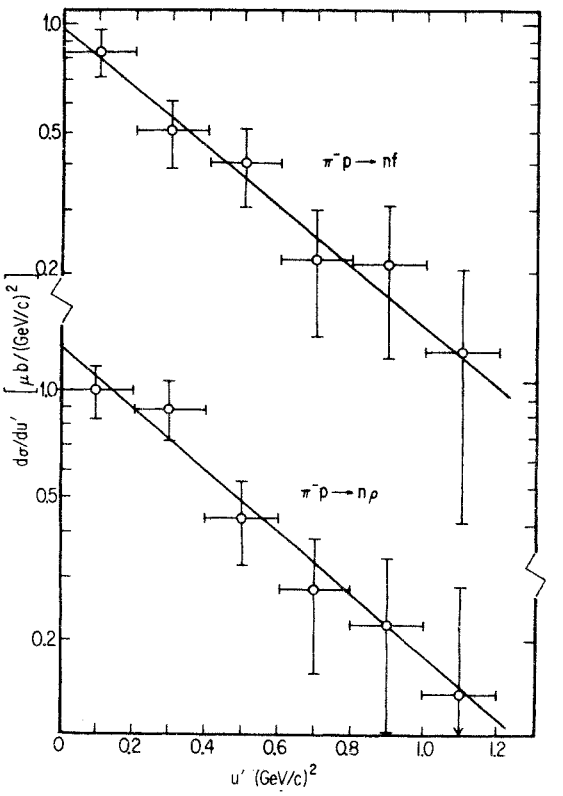

Fig.2

We may compare these results with other experiments at different energies /3-7/. Figure 3 shows the slope B of $d\sigma/du'$ plotted against s for ρ's and f's. Our experiment confirms the shrinkage of the background peaks suggested by the earlier experiments. We find that the slopes are roughly linear in $\ell n(s)$ (ignoring the point of Reference 5 for ρ's) with slope 1.4 ± 0.4 $(GeV/c)^{-2}$ for ρ's and 1.3 ± 0.4 $(GeV/c)^{-2}$ for f's. Figure 4 summarizes the intercept of $d\sigma/du'$ $(u'=0)$ for ρ production. A fit to the form s^{-n}

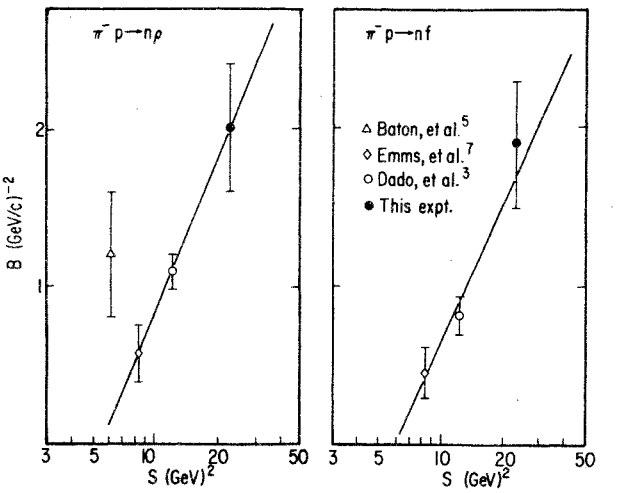

Fig.3

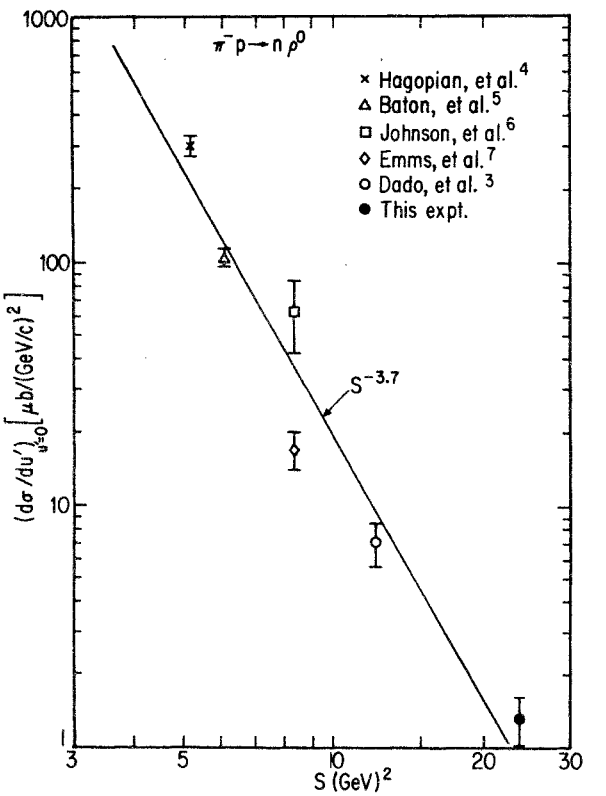

Fig.4

yields $n=3.7\pm0.1$. A fit to s^{-n} for f production in Figure 5 yields $n=3.4\pm0.3$. We note the similar s dependence for both the ρ and f. This result is striking in view of the fact that N exchange is allowed in both ρ and f production whereas exchange is allowed only in ρ production.

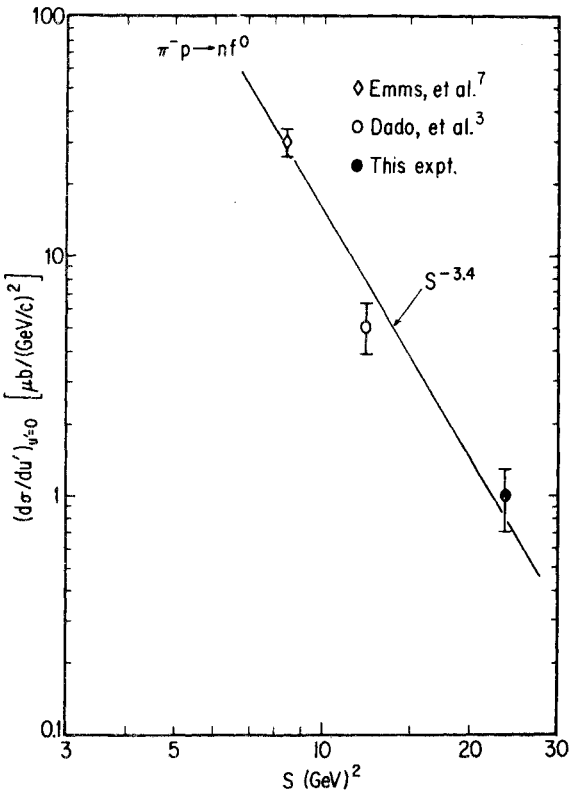

Fig.5

We thank the many people at the Stanford Linear Accelerator Center who have helped to make this experiment possible. We are expecially grateful for the helpful encouragement of Dr. J.Ballam. Gordon Bowden and the 40" bubble chamber crew made the bubble chamber an extraordinary success. Dauna Whitehead and our scanning staff deserve special acknowledgment for their efficient and dedicated work.

References

1. E.W.Anderson et al., Physical Review Letters 22, 102 (1969).
2. E.W.Anderson et al., Physical Review Letters 22, 1390 (1969).
3. S.Dado et al., Physics Letters 50B, 275 (1974).
4. S.Hagopian et al., Physical Review Letters 24, 1445 (1970).
5. J.P.Baton and G.Laurens, Nuclear Physics B21, 551 (1970).
6. P.B.Johnson et al., Physical Review 176, 1651 (1968).
7. M.J.Emms et al., Physics Letters B51, 195 (1974).

SMALL MOMENTUM TRANSFER ANTIPROTON CHARGE EXCHANGE SCATTERING ON PROTONS AT 30 GEV/C

V.V.Isakov, D.B.Kakauridze, G.V.Khaustov, V.E.Pestoev, Yu.D.Prokoshkin, A.V.Startsev

Institute for High Energy Physics, Serpukhov, USSR

The investigation of antiproton charge exchange scattering on protons

$$\bar{p}p \to \bar{n}n \qquad (1)$$

is of great interest both from the point of view of studying the energy dependence of a narrow forward peak at small momentum transfers[1-3] and a detailed study of the structure in the differential cross sections which we observed at $p = 40$ GeV/c[4].

It is also of interest to carry out a simultaneous analysis of reaction (1) abd cross-symmetric process

$$n + p \to p + n \qquad (2)$$

that was experimentally studied in the same energy range[5].

In the present work reaction (1) was investigated with 30 GeV/c antiprotons at the IHEP accelerator. The experimental set-up consisted of the same basic elements as in the earlier experiment[4]: i.e, a system scintillation and threshold Čerenkov counters used to define the beam and identify particles; a liquid hydrogen target, surrounded by a guard counter system which allowed one to suppress effectively charged particles and photons, produced from antiproton interaction in the target; a system of scintillation hodoscope counters used to determine the angle and the point of the incoming particle; a spark detector, consisting of wide-gap spark chambers, alternated by iron plates with a full thickness of 3 collision lengths or 25 radiation lengths. The spark detector was used to identify antineutrons by their nuclear interpretation in the steel plates of the spectrometer. A magnet was introduced between the target and the spark detector to deflect a charged particle beam from the spectrometer. 12 000 events of charge exchange reaction (1) were recorded in the experiment.

The angular distribution for reaction (1) obtained experimentally at p = 30 GeV/c is presented in Fig. 1. The resolution of the set-up over the 4-momentum transfer squared was better than 10^{-3}(GeV/c)^2 at $t \simeq 0$. With the growth of the error became larger: $\Delta t = 0.04\sqrt{-t}$ (in terms of (GeV/c)^2). As is seen from Fig. 1 in the range of momentum transfer $0 \leq t \leq 0.02$ (GeV/c)^2 there is a distinct narrow forward peak in the angular distribution for reaction (1). It is similar to the one observed at lower energies[1-3]. Further on with the increase of $-t$ one reveals a new structure in the distribution, i.e., after a sharp fall of the cross section at $-t = m_\pi^2$, it starts growing again, passes the maximum at $-t \simeq 0.05$ (GeV/c)^2 and then decreases exponentially with the slope $b \simeq 7$ (GeV/c)$^{-2}$.

Thus the experiment performed by our group, confirmed the existence of a structure at small angles in the angular distribution of reaction (1) at high energies observed at p = 40 GeV/c[4]. The t-position of the dip and the second maximum in the angular distribution of the reactions observed at 30 GeV/c is the same as at 40 GeV/c.

References

1. P.Astbury et al. Phys.Lett., 23, 160 (1966).
2. W.Beush et al. XV Int. Conf. on High Energy Phys., Kiev (1970).
   W.Awood et al. Phys. Rev., 2, 2519 (1970).
3. J.G.Lee et al. Nucl.Phys., B52, 292 (1973).
4. V.N.Bolotov et al. EPS Int. Conf. on High Energy Phys., Report L-61, Palermo (1975).
5. A.Babaev et al. EPD Int. Conf. on High Energy Phys., Report 62-02, Palermo (1975).

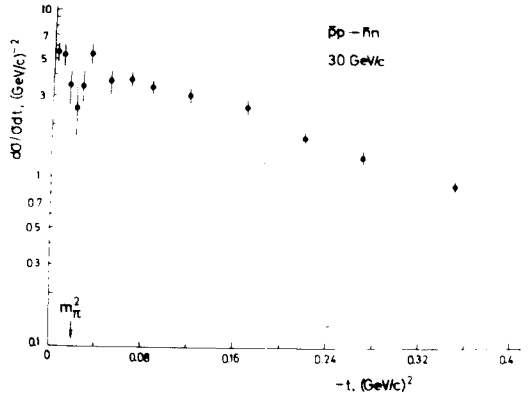

Angular distribution for charge exchange reaction (1) at 30 GeV/c.

THE MEASUREMENT OF NUCLEON-NUCLEUS INELASTIC CROSS SECTIONS AT ENERGIES HIGHER THAN THOSE OF ACCELERATORS

R.A.Nam, S.I.Nikolsky, N.I.Starkov, V.A.Tsarev, A.P.Chubenko, V.I.Yakovlev

P.N.Lebedev Physical Institute, Moscow, USSR

The cosmic ray hadrons with 1000-30000 GeV energy were selected by the ionization calorimeter of Tien-Shan EAS complex[1]. If such hadron is not accompanied by an air shower, it is a primary proton passing through the atmosphere without inelastic collisions. The extensive air showers accompanying hadrons were detected by hodoscopic counters and scintillators. There were registered the air showers with a number of electrons at the measurement level (700 g/cm^2) more than $\sim$100.

The flux of surviving primary protons $I(E,x)$ is connected with the primary flux $I(E,0)$ by the relation

$$I(E,x) = I(E,0)\exp(-x/\lambda).$$

where $\lambda = A/M\,\sigma_{p\text{-}air}$, $\sigma_{p\text{-}air}$ is the nucleon - air nucleus inelastic cross section, A is the air average atomic weight, M is Avogadro number, the thickness of atmosphere x =700 g/cm^2. The primary energy spectrum of protons is established well up to energy $\sim 10^{12}$ eV [2]. The extrapolation of this spectrum in the energy region 10^{12}-10^{14} eV coincides with the energy spectrum obtained by indirect methods of the extensive air showers[3].

To compare the experimental data and the theoretical extrapolations of the total pp-cross section in high energy region we used different forms of extrapolation.

1. $\sigma_{tot} = 38.4 + 0.5\,\ell n^2(s/137)$ mb [4,5]
   $\ell = 12.8$ (Gev/c)^2
2. $\sigma_{tot} = 27.2\,s^{0.06}$ mb [6]
   $\ell = 12.8$ (Gev/c)^2
3. $\sigma_{tot} = 27.1 + 1.78\,\ell n\,s$ mb [7,8]
   $\ell = 10.9 + 0.24\,\ell n\,s$ (Gev/c)^2

4. $\sigma_{tot} = 40.77 + 2.42\cos(-0.1 + 0.68\ln s) + 0.05 s^{-0.5}$
$b = 10.9 + 0.1\ln s - 1.2\sin(0.6\ln s)$ $(Gev/c)^2$ /7/

5. $\sigma_{tot} = 73 - 325/\ln(s/0.11)$ mb
$b = 8.32 + 0.57\ln s$ $(Gev/c)^2$ /9/

Here b is the slope parameter of elastic pp-scattering differential cross section. We assume that the Glauber theory is applicable to the region of high energies with certain modifications due to inelastic shadowing account taken into consideration.

The comparison of the experimental data to the calculated curves for the different (1-5) dependences of interaction cross section on the energy can be seen in fig.1. Our experimental data for protons with energy 1500-4000 GeV are corrected on the calculated events with small shower accompaniment. This correction is shown

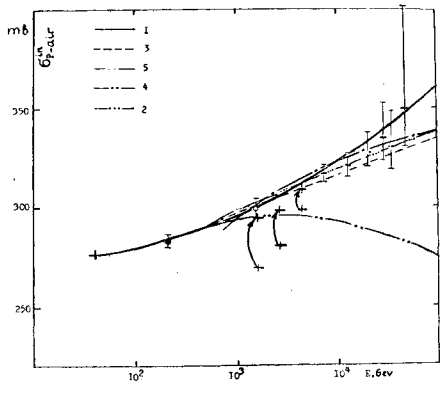

Fig.1

in the figure. Our experiment gives the proton-lead nucleus inelastic collision cross sections for different energies obtained from the distribution of the interaction points in lead absorber of the ionization calorimeter. This data ($\sigma_{p-Pb} = 1880 \pm 20$ mb for $\langle E_p \rangle = 4500$ GeV) do not contradict to the increase of inelastic collision cross section but this result is less certain than those for air because the different theoretical models are less distinguished in σ_{p-Pb}. The general result of the work is the conclusion about the increase of nucleon- nucleus inelastic collision effective cross section at the energies exceeding those of accelerators. The comparison with calculation shows that most acceptable are models with the σ_{tot} dependence of $\ln^2 s$, $\ln s$ and $s^{0.06}$ type.

References

1. T.P.Amineva, V.S.Aseykin et al. Trudy FIAN, v. 46, 157 (1972).
2. M.J.Ryan et al., Phys.Rev.Lett., v.28, N 5, 985 (1972).
3. S.I.Nikolsky, preprint FIAN No 35 (1970).
4. H.Cheng, J.K.Walker, T.T.Wu, Phys.Lett., 44B, 97 (1973).
5. L.D.Soloviev, A.V.Shelkachev, Yadernaya Fizika v.23, 636 (1976).
6. S.Y.Chu, B.R.Desai et al., preprint OCR-75-03 (1975).
7. N.P.Zotov, N.I. Starkov, V.A.Tsarev. JETP Letters 18, 460 (1973). Kratkie Soobsheniya po Fizike, N 12, 3 (1975).
8. A.J.Buras, J.Dias de Deus, Nucl. Phys. 71B, 481 (1974).
9. R.J.N.Phillps , Proc. Int. Conf. on Element. Particles, Amsterdam (1972).

ТЕОРИЯ ПОМЕРОНА С $\alpha > 1$ И ДИНАМИКА ФРУАССАРОНА

К.А.Тер-Мартиросян

Институт теоретической и экспериментальной физики, Москва

Этот краткий обзор основан на работах[1,2,3] группы МФТИ-ИТЭФ-Дубна. Речь идет о теории померона с $\alpha > 1$[4,5], удовлетворяющей s и t унитарности и описывающей данные опыта с малыми $p_\perp$. Идея состоит в введении P-траектории $\alpha(t) = 1 + \Delta + \alpha' t$, вклад которой $M_P \simeq i g_A g_B e^{(\Delta - \alpha' q_\perp^2)\xi_1}$, $\xi_1 = \xi - \frac{i\pi}{2}$, $\xi = \ln \frac{s}{2m^2}$, растущий как s^Δ, сокращается в эйкональном ряде

$$M(\xi, q_\perp) \simeq i g_A^0 g_B^0 e^{\xi_1 \Delta} \sum_{n=1}^{\infty} C_n \frac{(-z)^{n-1}}{n\,n!} e^{-\lambda q_\perp^2 / n} \qquad (I)$$

вкладом последовательных перерассеяний (рис.1). Здесь $z = g_A^0 g_B^0 e^{\xi_1 \Delta}/\lambda$, $\lambda = \alpha' \xi_1 + R^2$, $g_A = g_A^0 \exp(R_A^2 t)$, $R^2 = R_A^2 + R_B^2$, а $C_n = N_n^A N_n^B / (g_A^0 g_B^0)^n$ – безразмерные коэффициенты. Амплитуду (I), приводящую к наблюдаемому на опыте росту σ_{tot}, переходящему во фруассаровский ход $\sigma_{tot} \sim \pi a_0^2 \xi^2$ при $\xi \gg 1/\Delta$, будем называть фруассароном(нулевого порядка). В (I) она записана без учета усиленных графиков. Ниже показано, что

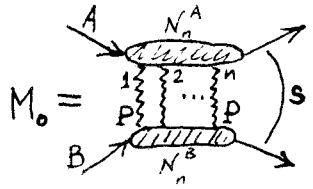

Рис.I.

(а) их учет не приводит к нарушению s-унитарности и (в) фруассарон (I) хорошо описывает все известные сейчас данные опыта.

Анализ удобно проводить в представлении прицельного параметра $\vec{\rho}$, характеризуя амплитуду функцией профиля рассеяния

$$F(\xi, \rho) = 1 - e^{2i\delta(\xi,\rho)} = \int_0^\infty \frac{2}{i} M(\xi, q_\perp) J_0(\rho q_\perp) q_\perp \, dq_\perp$$

Вклад померона в этом представлении $F_P = f(\xi, \rho)$ есть $f = z\, e^{-\rho^2/4\lambda}$, причем $f = 1$ при $\xi > 1/\Delta$ при $\rho = \rho_0$, где $\rho_c = a_c \xi - \rho_c \ln \eta_c \xi$, причем $a_0 = 2\sqrt{\alpha'\Delta}$, $\beta_0 = \sqrt{\alpha'/\Delta}$. Фруассарон (I) имеет в нем форму

$$F_0(\xi, \rho) = \sum_{n=1}^{\infty} (-1)^{n-1} C_n f^n(\xi, \rho)/n! \simeq 1 - e^{-f(\xi,\rho)} \qquad (2)$$

отвечающую кривой рис.2. Последнее видно из

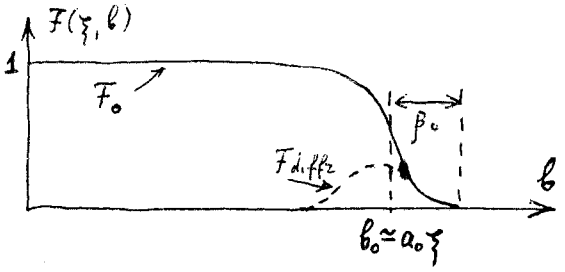

Рис.2.

анализа различных физически разумных приближений: модели эйконала, полагающей $C_n \equiv 1$ и дающей $F_0 = 1 - e^{-f}$, или более аккуратной модели рождения резонансов при перерассеяниях на померон, дающей $F_0 = 1 - \sum_n B_n e^{-D_n \nu}$, где B_n и D_n – некоторые коэффициенты, причем $\sum_n B_n = 1$ (и $\sum_n B_n D_n = 1$). В общей форме: $F_0 = E(f)$, где $E \to 1$ при $f \to \infty$ и $E \to \nu$ при $\nu < 1$, или, как показал Карди[6],

$$F_0(\xi, \rho) = C_0 \theta(\rho_0 - \rho), \qquad (3)$$

если C_n в (2) являются значениями аналитической функции $C_n = C(n)$, не растущей при $n \to \infty$ быстрее экспоненты. Как видно из рассмотренных примеров, должно быть $C_0 = C(0) = 1$, а θ – функция должна быть "сглажена" на длине $\Delta\rho \sim \beta_0$.

Отметим, что пороговые особенности (при $t = -q_\perp^2 \to 4\mu_\pi^2$) амплитуды немного меняют эти выводы, – в частности, профиль рис.2 на его "хвосте" (при $\rho \gtrsim a_0 \xi$), немного изменяя величины a_0 и β_0. Однако для дальнейшего это не важно, как не важна также и явная форма функции $F_0 = E(f)$, которую мы будем брать в простейшем виде $1 - e^{-f}$.

Вводя все многомерные взаимодействия

$$\mathcal{L}' = \sum_{n,m} (-1)^{n+m} g_{nm} \frac{\varphi^n \bar{\varphi}^m}{n!\,m!}$$

и полагая, что вершины $g_{nm} = g(n,m)$ аналитичны в n, m и не растут при $n, m \to \infty$ быстрее экспоненты, получим вклад усиленного

графика рис.3 с двумя "струями" померонов в виде[6]

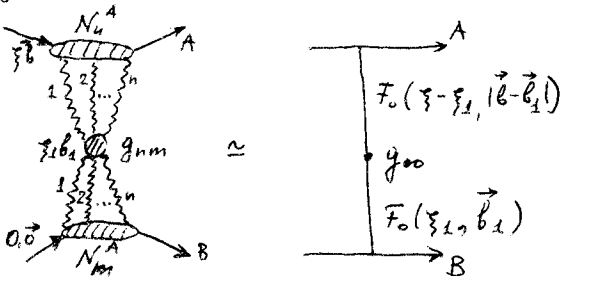

Рис.3.

$$\delta F(\xi,\ell)=\int\frac{d^2\ell_1}{4\pi}\int_0^{\xi}F_0(\xi-\xi_1,|\vec{\ell}-\vec{\ell}_1|)\,g_{00}\,F_0(\xi_1,\ell_1)\,d\xi_1,$$

где $g_{00}=g(0,0)$ есть константа размерности $1/см^2$. Точно также, суммируя по числам n_k померонов в каждой померонной "струе", можно определить амплитуду в виде суммы вклада всех усиленных графиков рис.4, построенных на линиях распространения фруассаронов - $F_0(\xi,\ell)$ и на вершинах g_{00} их взаимодействия. В каждой вершине может сходиться любое их число, причем ее вклад

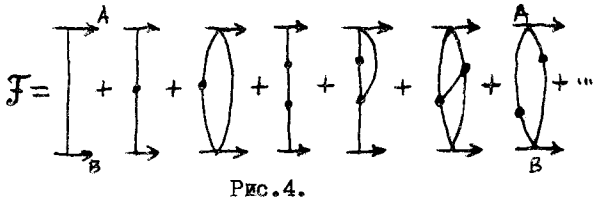

Рис.4.

остается равным g_{00} (этот результат, справедливый[6] при $\xi\to\infty$, такой же, как если бы g_{nm} имело вид $g_{00}G^{n+m}$, где G -некоторая константа). Линии двух или нескольких фруассаронов на рис. 4 не могут оканчиваться в одной точке, если они все начались в одной другой. Если бы $F_0(\xi,\ell)$ была θ - функцией (3) с резким краем, то вклады графиков рис.4в и рис. 4с (как и рис. 4d и рис.4е) точно взаимно сократились[6]. Фактически это сокращение происходит лишь частично и возникает задача получения вклада $F(\xi,\ell)$ всех "усиленных" графиков рис.4. Отметим, что этот вклад $F(\xi,\ell)$ (точный фруассарон) удовлетворяет уравнению

$$F(\xi,\ell)=E(V)\simeq 1-e^{-V}, \qquad (4)$$

$$V(\xi,\ell)=P(\xi,\ell)+C(\xi,\ell)+D(\xi,\ell), \qquad (5)$$

где $C(\xi,\ell)$ - есть суммарный вклад всех графиков типа цепочки рис.5, состоящих из звеньев $Z(\xi,\ell)$, с числом более двух, связанных вдоль t -канала лишь вершинами g_{00}, причем $Z=F(\xi,\ell)-C(\xi,\ell)$. Через $D(\xi,\ell)$ обозначен вклад графиков, "неприводимых" по t- и по s-каналам,- в том смысле, что они не являются ни

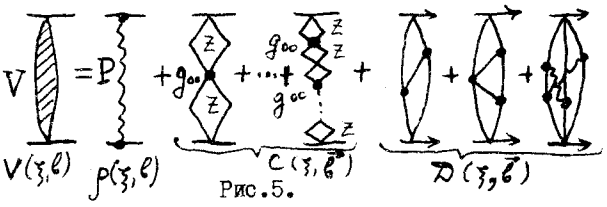

Рис.5.

цепочкой, как $C(\xi,\ell)$ (в t-канале), ни состоят из эйкональной цепочки, (в s-канале), составленной из других графиков. Примеры указаны на рис.5, они построены из линий точного фруассарона $F(\xi,\ell)$ и вершин g_{00}, в каждой из которых сходятся не менее трех линий фруассаронов. В $\omega\vec{q}_\perp$-представлении вклад цепочки $C(\xi,\ell)\to C(\omega,K)$ может быть выражен через точный фруассарон $F(\xi,\ell)\to\varphi(\omega,k)$

$$C(\omega,k)=g_{00}\varphi^2(\omega,k)/(1+g_{00}\varphi(\omega,k)) \qquad (6)$$

Равенства (4)-(6) вместе с представлением $D(\xi,\ell)$ на основе правил Грибова[7] в виде вклада графиков рис.5 является интегральным уравнением для функции $\varphi(\omega,k)\to F(\xi,\ell)$.

Так как $C(\xi,k)$ - величина порядка g_{00}, при $g_{00}\to 0$, а $D(\xi,k)$ - порядка g_{00}^2, то при малых g_{00} решение уравнения можно получить методом итераций, полагая в нулевом приближении $g_{00}=0$, т.е. $F\simeq F_0(\xi,\ell)$, где F_0 - есть функция (2), (3). При $\omega>a_0q_\perp$ (когда важна, как можно показать, область $\ell\ll a\xi$) ей отвечает $\varphi_0(\xi,q_\perp)=(a_0/2)^2/(\omega^2+a_0^2q_\perp^2)^{3/2}$. При подстановке в (6) это приводит к полюсу Редже у $C(\omega,k)$ при $\omega=\omega_0=(\tilde{g}^{2/3}-a_0^2q_\perp^2)^{1/2}$, где $\tilde{g}=(a_0/2)^2g_{00}$. Это дает экспоненциально растущее с ростом ξ, отрицательное $C(\xi,\ell)$:

$$C(\xi,\ell)\simeq const\,\theta(\ell_0-\ell)\exp\left(\tilde{g}^{1/3}(\xi^2-\ell^2/a^2)^{\frac{1}{2}}\right).$$

Это значение справедливо при $\ell<\ell_0\simeq a_0\xi$, при $\ell>a_0\xi$ анализ требует учета пороговых особенностей амплитуды и дает аналогичные результаты. Сравнивая это значение $C(\xi,\ell)$ с вкладом $\int\sim e^{\xi\Delta-\ell^2/4\alpha'\xi}$ померона, получаем,

что $|C| < \rho$ в области $\ell < a_c \xi$ при условии $\tilde{g} = (a_c/2)^2 g_{cc} < \Delta^3$, т.е. при $g_{cc} < \Delta^2/\alpha'$. При этом и $D(\xi, \ell)$ может быть вычислено на основе теории возмущений и по модулю всегда меньше, чем ρ (оно не содержит опасно растущих при $\xi \to \infty$ членов). Поэтому при $g_{cc} < \Delta^2/\alpha'$ уравнение (4)-(6) может быть решено методом итераций и его нулевым приближением, заведомо справедливым при достижимых энергиях является нулевой фруассарон $\mathcal{F} = \mathcal{F}_0(\xi, \ell)$.

Покажем кратко, что эта амплитуда (I)-(2) хорошо описывает все известные сейчас данные опыта для небольших $p_\perp$ (коэффициенты C_n можно брать в виде "квазиэйконала" $C_n \simeq C^{n-1}$ или учитывать возможность рождения резонансов при каждом перерассеянии; от выбора их результаты зависят слабо).

I) Полное сечение σ_{tot} и наклон конуса B определяются согласно (I) формулами

$$\sigma_{tot} = 8\pi \, Re\,[g_A^0 g_B^0 e^{\xi_1 \Delta} f(z)]$$

$$B = 2\, Re\,[(\alpha' \xi_1 + R^2) f_1(z)],$$

где $f(z) = \sum_{n=1}^{\infty} \frac{(-z_1)^{n-1}}{n \cdot n!}$, $f_1(z) = \sum_n \frac{(-z_1)^{n-1}}{n^2 \cdot n!} / f(z)$, $z_1 = C z$. Пренебрегая при $\xi > 1$ малой комплексной фазой функций f и f_1, получим

$$\sigma_{tot}' / \sigma_{tot} \simeq B'/B \simeq \Delta,$$

если $z'/z = 0$, т.е. при $\Delta = \alpha'/(\alpha' \xi + R^2)$, где штрих у σ_{tot} и B означает дифференцирование по ξ. Опыт показывает, что действительно $\sigma_{tot}'/\sigma_{tot} \simeq B'/B \simeq 0.07$ в области Батавии- ISR, где $\xi \simeq \xi_0$, $\xi_0 = 6$. Это соотношение называют геметрическим скейлингом. Таким образом, $\Delta = 0{,}07$, а $\alpha' = (\alpha' \xi_c + R^2)\Delta$, так как $\alpha' \xi_0 + R^2 \simeq B/2 f_1(z) \simeq B/2.4$ ($f_1(z)$ близко к I.I-I.2), а $B \simeq$ I2-I4, то $\alpha' = 5\Delta \simeq 0.35$ (Гэв/с)$^{-2}$. Так как $\alpha' \xi_c + R^2 = 5$, то $R^2 \simeq 5 - 2.5 \simeq 3$(Гэв/с)$^{-2}$, причем отношение $\sigma_{tot}/B = \mathcal{F}(z)$ определяет величину z, т.е. вычет $g_A^c g_B^c$ померона. Более точные значения Δ, α', R^2 и $\gamma_c = g_A^c g_B^c$ (вместе с параметрами f, ω, ρ, A_2 полюсов, дающих небольшие поправки), соответствующие лучшему описанию эксперимента (рис.6,7,8), указаны в табл. I.

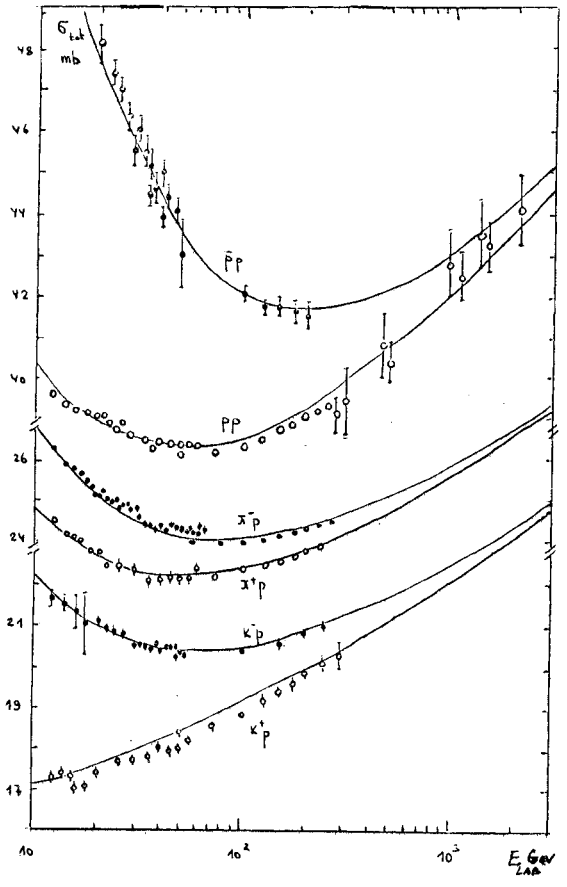

Рис.6.

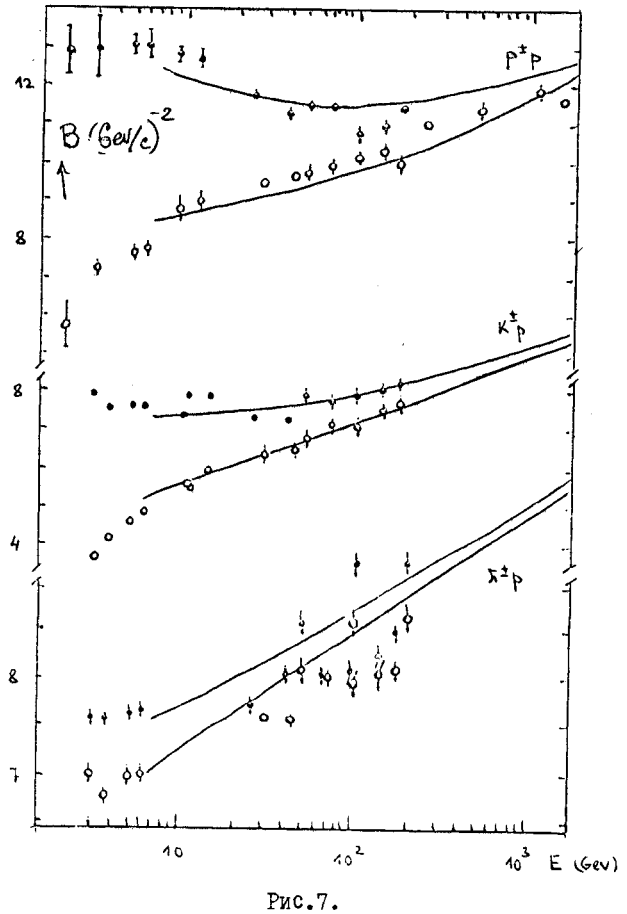

Рис.7.

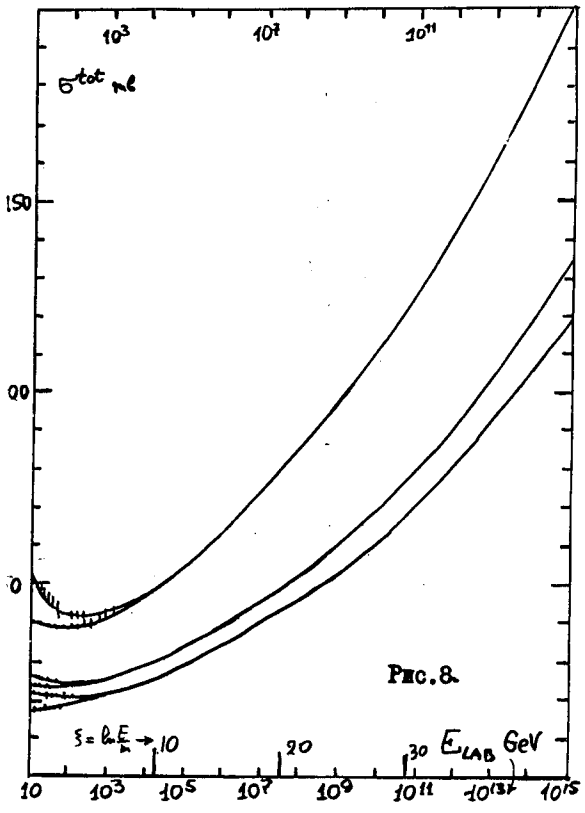

Рис.8.

Таблица I. $g_{NR}(q_\perp^2) = g_A^{(1)} e^{-R_1^2 q_\perp^2} + g_A^{(2)} e^{-R_2^2 q_\perp^2}$

$g_{Aa}(q_\perp^2) = g_{Aa}^0 e^{-R_{Aa}^2 q_\perp^2}$

$a \to$		P	f	ω	ρ	A_2
$\alpha_a(0)$		I.062	0.45	0.43	0.49	0.35
$\alpha_a'(0)(Gev/c)^{-2}$		0.36	0.70	I.00	0.70	0.70
N	$g_N^{(1)}/g_N^{(2)}$	I.26/0.63	2.95	I.87	0.30	0.45
	$R_N^{(1)}/R_N^{(2)}$	2.32/-0.24	I.22	4.65	2.00	I.00
π	g_π^0	I.05	I.I4	-	I.47	-
	R_π^2	0.85	0.50	-	3.I9	-
K	$g_K^{(0)}$	0.9I	0.5I	0.50	0.75	0.60
	R_K^2	0.44	0.30	0.65	2.00	I.00

В рассмотренном варианте теории сечения $\sigma_{tot} \simeq 2\pi R_o^2$, $R_o = a\xi$ безгранично растут при $s \to \infty$ (рис.8), показывая универсальный ход в области $\xi \Delta > 1$, для $E_{lab} \simeq 10^8 - 10^{10}$ Гэв, где они имеют огромные значения $\sigma_{tot} \sim 100$ мбн, при этом σ_{el} также растет, $\sigma_{el} \simeq \pi R_o^2$, достигая $1/2\ \sigma_{tot}$.

2) Для описания хода $d\sigma/dt$ (рис.9) в области не очень малых t ($|t| \lesssim 1$ Gev) померонную вершину нуклона пришлось представить в виде суммы двух экспонент.

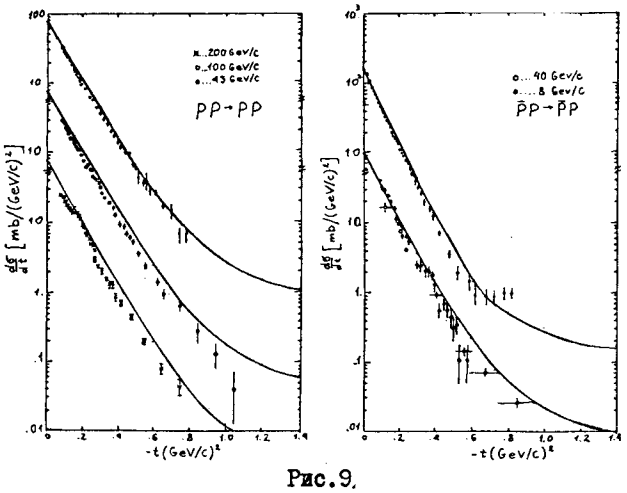

Рис.9.

3) Амплитуда процесса диффракционного рождения частиц $\mathcal{F}_{diffr} \simeq \rho(\xi, b) e^{-\rho(\xi b)}$ определяется кривой типа пунктира на рис.2, а его сечение отвечает площади кольца $\sigma_{diffr} \simeq 2\pi \beta_o R_o$, т.е. должно расти при $s \to \infty$ как $\xi \simeq \ln(s/2M^2)$.

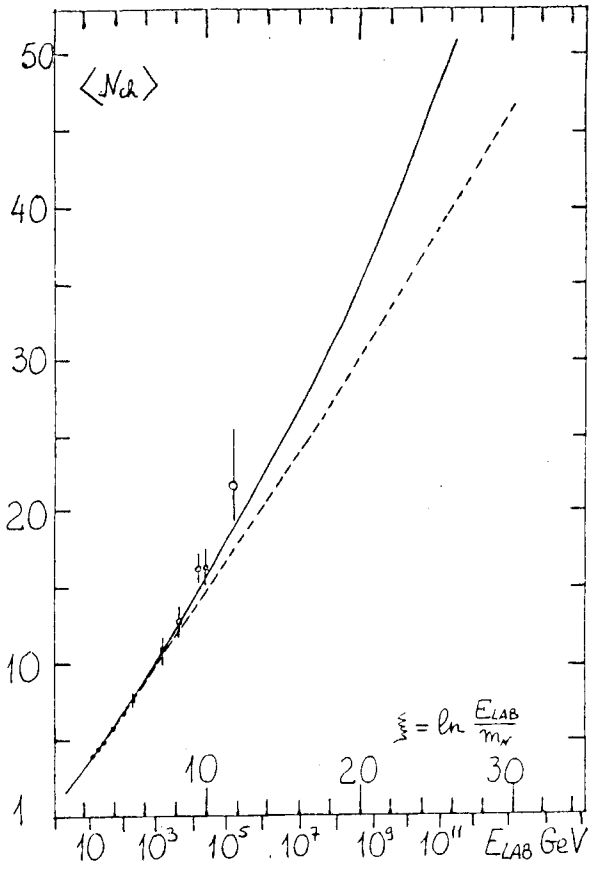

Рис.10.

4) Инклюзивное сечение $d\sigma_{inel}/dy$ и средняя множественность (рис.10) должны расти

при $S \to \infty$ по степенному закону $\sim S^{\Delta}$ — как среднее число померонов в эйкональном ряду (I)-(2).

Литература

1. M.S.Dubovikov, K.A.Ter-Martirosyan. Preprint ITEP-37, Moscow, 1976.
2. M.S.Dubovikov, B.Z.Kopeliovich, L.I.Lapidus, K.A.Ter-Martirosyan. Preprint JINR D2-9789, Dubna, 1976.
   B.Z.Kopeliovich, L.I.Lapidus, Preprint JINR, E2-9537, Dubna, 1976.
3. A.M.Lapidus, V.I.Lison, K.A.Ter-Matritosyan, P.E.Volkovitsky. Preprint ITEP 115, Moscow, 1976.
4. H.Cheng, T.T.Wu. Phys.Rev.Lett. 24, 1456, 1970.
5. A.Capella, J.Thank Tran Wan, J.Kaplan. Preprint LPTHE, Leningrad, 75/12.
6. J.L.Cardy. Nucl.Phys., B75, 413 (1974).
7. В.Н.Грибов. ЖЭТФ 53, 654 (1967).

THE DESCRIPTION OF THE LOW MULTIPLICITY REACTIONS

L.A.Ponomarev

ITEP, Moscow, USSR

I will consider briefly the theoretical description of the diffractive dissociation (DD) data in the reactions

$$a + N \to a + (N\pi), \qquad (1)$$

$$\pi^{\pm} p \to \pi^{\pm}(\Delta^{++}\pi^{-}),\ \pi^{+}p \to (\pi^{+}p^{0})p. \qquad (2)$$

As for reaction (1), the different theoretical approaches may be classified by means of Feynman graphs in Figs. 1-4.

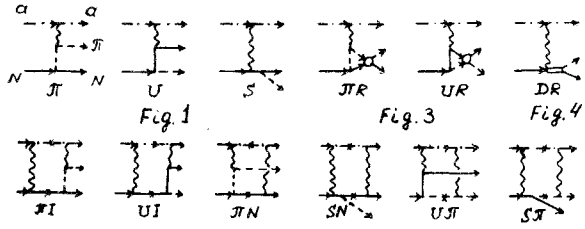

Fig. 1 Fig. 3 Fig. 4

Fig. 2

The wavy, dotted and unbroken lines correspond to the reggeon (as a rule to the pomeron), pion and nucleon accordingly. Fig. 1 contains the pion pole graph and U-channel and S-channel nucleon graphs; Fig. 2 contains rescattering graphs in onshell approximation; and Fig. 4 contains the graph which corresponds to the direct production of the resonances.

The whole amplitude containing all the mechanisms in Figs.1-4 has not been considered in the papers contributed to the Conference. But the majority of them was discussed in different papers.

The complete set of the variables is the following: M is the mass of the excited system, t is the momentum transfer to the excited system, z_t and φ_t are the cosine of the polar angle and the azimuthal angle in Gottfried-Jackson frame.

Let us consider amplitude which corresponds to the ordinary Deck mechanism and is used in the article[1]. First Deck model with reggeized pion exchange was considered by Berger[2].

The analogous model was suggested in ITEP[3].

I want to emphasize the following deficiency of this description:

a) The maximum in the mass distribution is very near to the threshold.

b) The break in the t-distribution in the region $-t \simeq 0.2 \div 0.4$ GeV^2 is absent.

c) The theoretical curves for angle distributions show no bump in the region $z_t \simeq -1$ and distribution is too asymmetrical.

Two distributions from ref.[1] are shown in Fig. 5 for example. The natural next step in

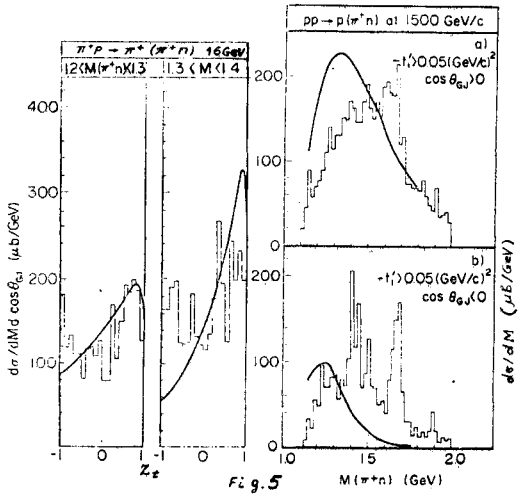

Fig. 5

the development of the DD theory is the model with all pole graphs in Fig. 1. This model without off-shell corrections was qualitatively considered in ref.[4]. In this work it was shown analytically that the differential cross section $d^3\sigma/(ds_1\,dt_1\,dt_2)$ has zero in low M and low $|t|$ region. The data (see Fig. 8a) confirm this conclusion. But our quantitative calculations in this model (see curve 2 in Fig. 8a) do not confirm this qualitative consideration. Fig. 8a shows that the theoretical cross section 3–4 times exceeds the data. To decrease the theoretical result for the absolute value of the cross section we considered this model with off-shell corrections[5]. Some distributions from this paper are displayed in Fig. 6. The conclusions from this work are:

a) The maximum from the mass distribution shifts to the high mass region in the coincidence with data. In the low mass region $M<1.3$ GeV there is large destructive interference of π and $(U+S)$ amplitudes.

b) The cross-over effect is obtained taking into account total amplitude $\pi+U+S$ only.

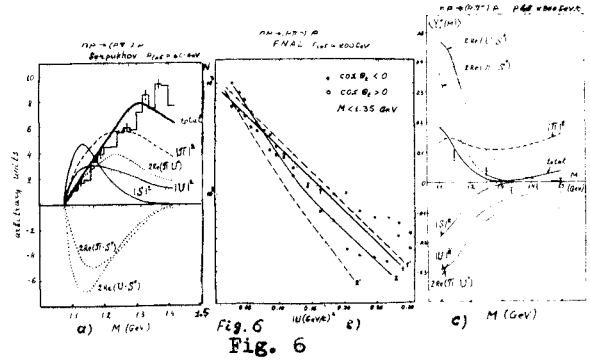
Fig. 6

c) It is necessary to use nucleon graphs to describe the maximum in distribution in the region $z_t \simeq -1$ and small mass of the excited system.

d) In spite of the naive expectation[7,8] in the model with spin taken into account the second bump in φ_t-distribution ($z_t \simeq -1$, $\varphi_t \simeq \pi$) is absent. This result was obtained in paper[9] in the analogous model.

e) But the absolute value of the cross section in the model keeps to exceed the data in this model.

The problem with absolute normalization may be solved by means of the rescattering graphs in Figs.2,3. First this is the model in which the amplitude without baryon exchange is considered and which was obtained by Tsarev[10] and later by Berger and Pirilä[11]. In paper[12] the model was developed which contains the amplitudes π, $\pi I + \pi N, \pi R$ and DR with reggeized pion exchange. The comparison of this model with the data[13] is shown in Fig. 7.

The coincidence of the theory with the data is satisfactory at this energy (P_{lab}=16 GeV/c). In paper[14] the amplitude was considered which contains the amplitudes π, U, πI and UI. The off-shell correction was taken into consideration by means of the phenomenological formfactors. The coincidence of the theory and the

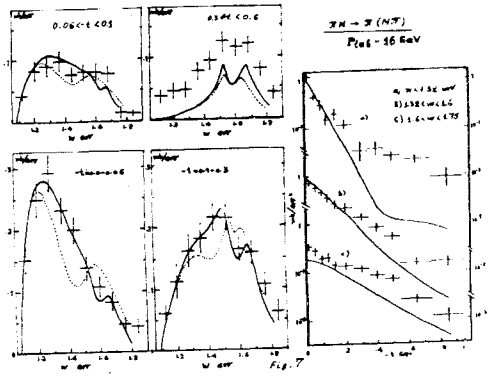

Fig. 7

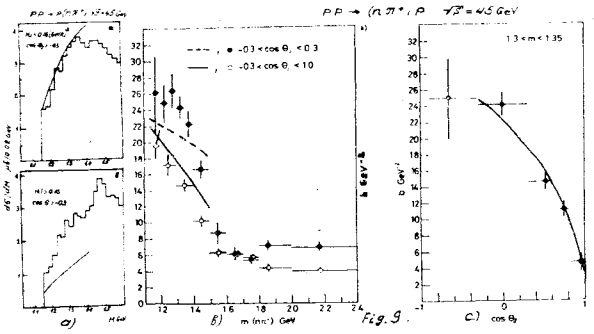

Fig. 9

data at high energies is not satisfactory. The main lack of this model is the absence of the S-channel nucleon graph and the interference terms which are rather large[5].

Let us consider the model with the amplitude $T = \pi + U + S + 2\pi I$. Factor 2 corresponds to the calculation of the amplitude πN, so $\pi I \simeq \pi N$. We can expect that the region of the applicability of our formulas is $x_t \geq 0$ (we do not consider amplitudes UI and SN) and the region of the low mass of the excited system (we do not consider amplitudes R, UR and DR). As for amplitudes $U\pi$ and $S\pi$ the estimate shows that its contribution is small. We do not consider off-shell correction in our model, so our model has no free parameters. Figures 8-9 contain the comparison of the model with ISR data[15,16]. The dotted curves in Fig. 8 correspond to the different amplitudes.

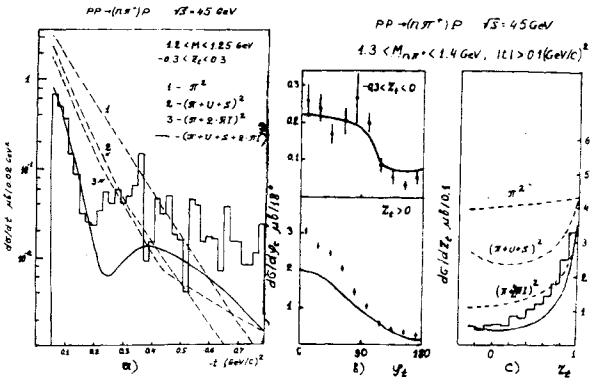

Fig. 8

Fig. 8 shows that: the absorption amplitude πI and amplitude $(U+S)$ have the same sign; the dip in $d\sigma/dt$ distribution in the region $|t| \simeq 0.2$ (Fig. 8a) may be explained only by means of the total amplitude and connects with interference term $\pi I(U+S)$.

Now I will consider briefly the reactions $\pi^+ p \to (\pi^+ \rho^0) p$ and $\pi^\pm p \to \pi^\pm (\Delta^{++} \pi^-)$. The qualitative analysis which was performed by Berger[1] predicts large contribution of u-channel graphs into these reactions (ρ exchange into $\pi^+ p \to (\pi^+ \rho^0)$ and Δ exchange into $\pi^\pm p \to \pi^\pm (\Delta^{++} \pi^-)$). But quantitative description of this reaction in the framework of the reggeized one-pion exchange model[1] shows that latter do not exceed 20%.

Conclusions:

1) There is large contribution of the different mechanisms (pion and nucleon exchange and absorption) and the interference terms in DD processes $aN \to a(N\pi)$.

2) The whole description of all phenomena in DD processes now is absent.

3) But the many characteristic features of the DD processes can be described in the simple models.

4) The contribution of the u-channel graphs into the processes $\pi^\pm p \to \pi^\pm (\Delta^{++} \pi^-)$ (Δ^{++} exchange) and $\pi^+ p \to \pi^+ \rho^0 p$ (ρ exchange) does not exceed 20%.

References

1. T.Hirose, K.Kanai and T.Kobayashi, Paper 406/A1-110, submitted to this conference.
2. E.L.Berger, Phys.Rev.Lett., 21, 701, 1968.
3. K.G.Boreskov, et al. Yad.Fiz. 15, 361, 1972.
4. F.Hayot, A.Morel, A.Stantoro and M.Souza, Paper 1211/A1-164, submitted to this conference.
5. L.A.Ponomarev, Paper 33/A1-33, submitted to this conference.
6. Babaev et al. Paper 28/A1-28, submitted to this conference.
7. J.Biel et al., paper submitted to the Palermo conference, 1975.
8. H.I.Miettinen, Plenary Session Talk on the Conference on High Energy Physics, Palermo, 1975.
9. A.Minaka, H.Sumiyoshi, M.Uehara, paper 371/A1-86, submitted to this conference.
10. V.Tsarev, Phys.Rev. D11, 1864, 1975.
11. E.L.Berger and P.Pirila, Phys.Rev., D12, 3448, 1975.
12. M.Uehara, Paper 68/A1-68, submitted to this conference.
13. H.Grassler et al. Nucl.Phys., B95, 1, 1975.
14. H.R.Gerhold, W.Majerotto, Paper 393/A1-111, submitted to this conference.
15. C.Broll, Thesis, Orsay, 1976.
16. H. de Kerret et al. Paper 65/A1-65, submitted to this conference.
17. E.L.Berger, paper 1006/A1-145, submitted to this conference, Argonne preprint ANL-HEP--PR-75-06.
18. A.N.Kamalov, L.A.Ponomarev. Papers 32/A1-32 and 1038/A1-93, submitted to this conference and ITEP preprints ITEP-8, ITEP-75, 1976.

PLENARY REPORT

BINARY AND LOW MULTIPLICITY REACTIONS

A.B.Kaidalov

ITEP, Moscow, USSR

I. Introduction

Investigation of elastic, quasi two-body and low multiplicity reactions is one of the main sources of information on the mechanism of strong interaction at high energies.

Many interesting results in this field have been obtained since the time of the London Conference. New measurements of total cross sections, real parts of forward elastic amplitudes, differential cross sections of elastic reactions in large t-interval are performed and new interesting effects are found. Sections II and III are devoted to the discussion of these results. New information on the spin effects in the elastic NN-scattering is also discussed in Section III.

Theoretical approaches to the description of two-body reactions at high energies are reviewed in Section IV.

Experimental investigations of inelastic binary reactions revealed new (sometimes puzzling) features of these processes. Charge exchange reactions and two-body resonance production are considered in Section V.

In the past few years considerable progress has been achieved in the investigation of inelastic diffractive reactions. Section VI is devoted to the discussion of new results in this field.

Nearly one hundred and seventy experimental and theoretical papers, devoted to the study of binary and low multiplicity reactions, were submitted to this Conference. Because of the limited size of this report I'll discuss only some of the new experimental results, general features, which follow from the data and shortly mention on their theoretical interpretation. I wish to appologize to all those authors whose results will be out of scope of this report.

II. Total Cross Sections and Real Parts of the Forward Elastic Amplitudes

New data on the total cross section of pp-interaction in the ISR energy range[1] are submitted to the Conference. It is well known that the substantial rise of $\sigma_{pp}^{(tot)}$ was found in the previous measurements at ISR[2]. The previous results depend on the value of luminosity L, which was measured independently. New results are obtained with increased precision ($\pm 0.6\%$) by two methods. This gives the possibility to measure $\sigma_{pp}^{(tot)}$ in a way independent of L. These results are shown in fig. 1. The new points are

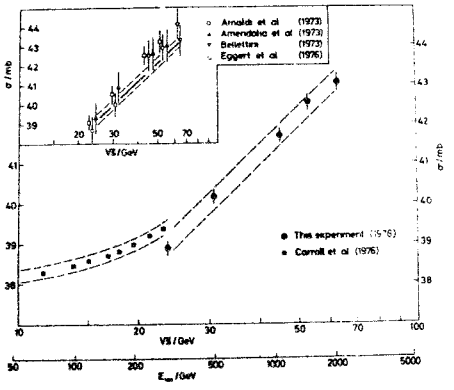

Fig. 1. $\sigma_{pp}^{(tot)}$ from paper[1] together with previous measurements[2] and FNAL data[3]. The broken lines represent the estimated scale error[1].

within the errors in an agreement with the previous data of ISR, though the new values of $\sigma_{pp}^{(tot)}$ at the highest ISR energies are systematically lower than the existed points. There is also some difference at the lowest ISR energy with the results from FNAL[3].

These measurements together with the previous results on the total cross sections of hadron-hadron interactions from FNAL[3] and Serpukhov[4] confirm the rise of all the $\sigma^{(tot)}$ at very high energies. On the other hand all the differences of particle and antiparticle total cross sections have the power law decrease with energy[3,4] in an agreement with Pomeranchuk theorem. It is of interest also to consider the energy dependences of the definite combinations of $\sigma^{(tot)}$, which correspond to the definite quantum numbers in t-channel (ρ, ω, A_2). For example

$$\Delta\sigma_{\omega}^{KN} = \frac{1}{4}\left[\left(\sigma_{K^-p}^{(tot)} - \sigma_{K^+p}^{(tot)}\right) + \left(\sigma_{K^-n}^{(tot)} - \sigma_{K^+n}^{(tot)}\right)\right], \qquad (1)$$

The values of $\Delta\sigma_{\omega}^{NN}$, $\Delta\sigma_{\omega}^{KN}$ and $\Delta\sigma_{\rho}^{\pi N}$ are shown in fig. 2. Note the universality of the $\Delta\sigma_i$ be-

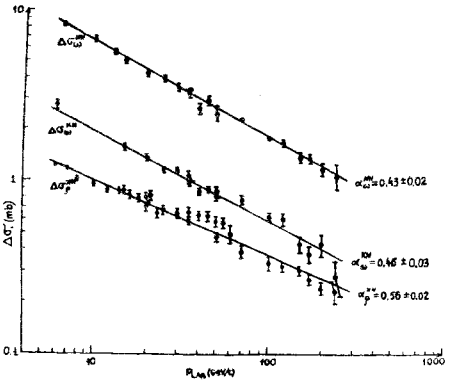

Fig. 2. $\Delta\sigma_{\omega}^{NN}$, $\Delta\sigma_{\omega}^{KN}$ and $\Delta\sigma_{\rho}^{\pi N}$ as functions of energy.

haviour, - the energy dependences of the contributions with the given quantum numbers are the same for different reactions. Thus for the parametrization $\Delta\sigma_i = A/p_L^{1-\alpha_i}$ the value of α_ω in NN($\bar{N}N$) interactions is $\alpha_{\omega}^{NN} = 0.435 \pm 0.02$ and $\alpha_{\omega}^{KN} = 0.45 \pm 0.03$. The values $\alpha_{\rho}^{\pi N} = 0.56 \pm 0.02$, $\alpha_{\rho}^{KN} = 0.55 \pm 0.12$, $\alpha_{\rho}^{NN} = 0.5 \pm 0.2$ are also equal within errors (α_ρ seems to be different from α_ω). It should be taken into account, that α_i are the intercepts of "effective" trajectories, which in general do not coincide with trajectories of Regge poles (because of the presence of Regge cuts). In the framework of the absorption model α_i^{eff} depend on energy (this does not contradict to the experimental data, which possibly indicate to some decrease of α_i^{eff} as energy increases) and at present energies $\alpha_i^{eff} - \alpha_i^{pole} \sim 0.1$. So the energy dependences of $\Delta\sigma_i$ show, that absorptive effects have universal character and $\alpha_{\rho}^{pole} - \alpha_{\omega}^{pole} = 0.1 \div 0.15$.

The results of the new measurements of the real parts of the forward elastic pp, $\bar{p}p$, π^+p, $K^\pm p$ -scattering are submitted to this Conference[5,6]. They are shown in fig. 3a)-d) together with the other new results[7,8].

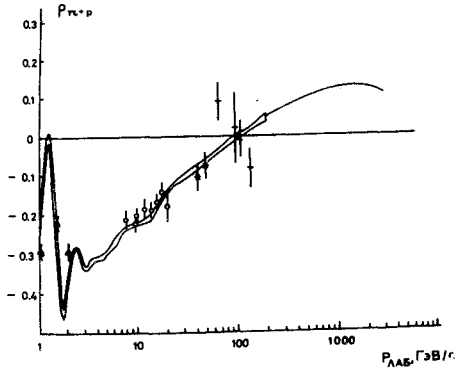

a)

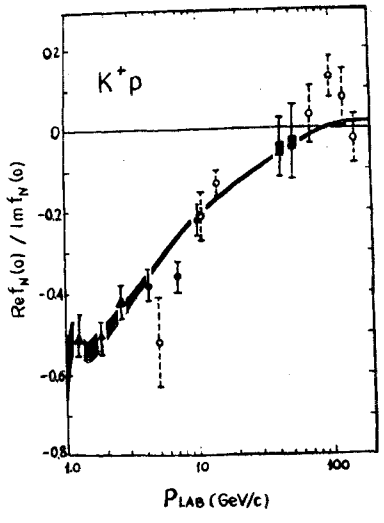

b)

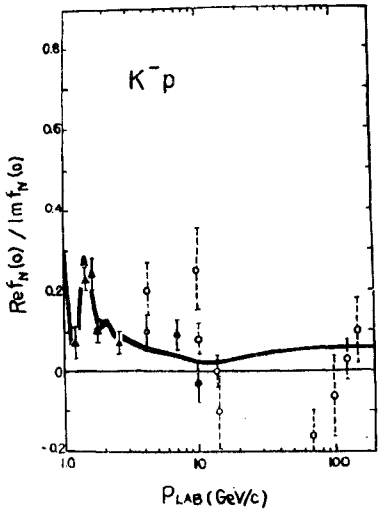

c)

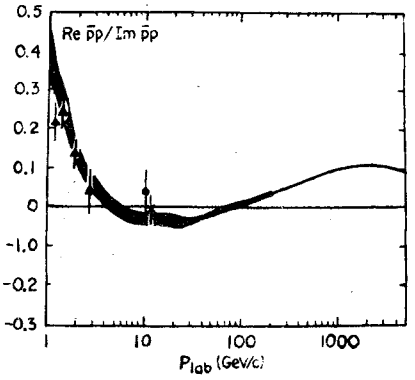

d)

Fig. 3. $\varrho = Re\,T(s,0)/Im\,T(s,0)$ for π^+p - a), K^+p - b), K^-p - c) and $\bar{p}p$ - d). Figures taken from ref./5-7/.

Previous information on the values of $\varrho = Re\,T(s,0)/Im\,T(s,0)$ for the reactions $K^\pm p$ and $\bar{p}p$ was very limited and rather contradictory. Functions ϱ in $\pi^\pm p$ and $K^\pm p$ -scattering probably change sign and become positive at energies $E_L \approx 100$ GeV. In K^-p -scattering ϱ is positive already at low energies. The predictions of dispersion relations are also shown in fig. 3. They are in good agreement with the new experimental data.

III. Elastic Scattering at Non-Zero Angles

In the past two years experimental information on the processes of elastic $\pi^\pm p$, $K^\pm p$, pp, np and $\bar{p}p$ -scattering at high energies substantially increased/9-20/ (especially in the region of $|t| > 1$ GeV^2).

Energy dependence of a diffraction slope b is shown in fig. 4 for different elastic reactions. Let us note, that the rise of the slope at $t = -0.2$ GeV^2 in pp-scattering is weaker than at $|t| < 0.1$ GeV^2 ($\alpha'(t=-0.2) = 0.13 \pm 0.02$/17/ and $\alpha'(t \approx 0) = 0.278 \pm 0.024$/21/). It is well known, that there is a substantial change of slope at $t \approx -0.15$ GeV^2 in elastic pp -scattering at ISR/22/. New very accurate measurements at SLAC/12/ have shown that the same structure exists in pp -scattering at energy 10 GeV. Interesting t-dependence of slopes was observed also

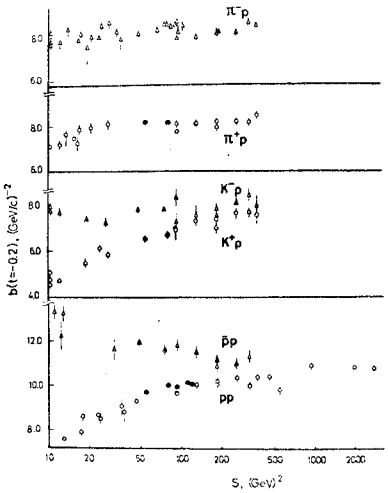

Fig. 4. The energy dependence of diffraction slope b (at $t = -0.2$). Figure taken from ref.[17].

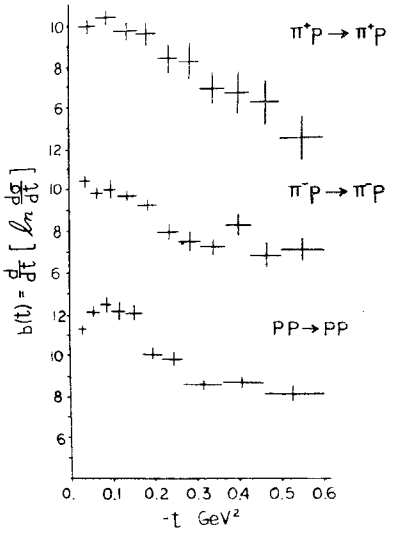

Fig. 5. The t-dependence of slopes of elastic π^+p, π^-p and pp-scattering at 200 GeV/c. Figure taken from ref.[20].

in other elastic reactions[12]. The t-dependence of slopes in $\pi^\pm p$ and pp-elastic scattering has been obtained in a high statistics experiment at 200 GeV[20] - fig. 5. The first time the decrease of the pp-slope is observed at very small values of t. This result is important for theoretical understanding of the structure of the diffraction cone.

Another interesting effect, - small oscillation of the differential cross section of elastic pp-scattering in the diffraction peak region, was observed at 60 GeV in Serpukhov[17]. The differential cross section was fitted by the smooth curve $\left(\frac{d\sigma}{dt}\right)_{fit} = \left(\frac{d\sigma}{dt}\right)_{t=0} \exp(bt+ct^2)$ x/. The difference $\frac{d\sigma}{dt} - \left(\frac{d\sigma}{dt}\right)_{fit}$ shown in fig. 6a, indicates to the existence of small oscillation with the period of ~ 0.4 GeV^2 and the scale of $\approx(0.05 \div 0.1)\frac{d\sigma}{dt}$.

Analogous phenomenon was observed also in the processes of the elastic α-nuclei scattering in Dubna at 18 GeV/c[23], fig. 6b)-d). Here the period of oscillation is much smaller. It means that the effect depends strongly on the radius of the system. The curves in fig. 6 are the calculations based on a simple theoretical model[24], which predicted the existence of these oscillations (see below).

The energy dependence of elastic cross sections at larger $|t|$ values is shown in fig. 7. The differential cross sections of π^-p and K^+p-scattering at fixed t-values practically do not depend on energy at $E_L \geq 30$ GeV. The cross sections of pp-scattering at fixed $|t| \gtrsim 1.2$ GeV^2 have minima in the FNAL energy range. Let us note that the elastic np-differential cross sections, measured in Serpukhov[15] in the region $|t| < 1$ GeV^2 coincide with $d\sigma_{pp}/dt$ at the same energies, however there is clear difference in magnitude and energy dependence of $\frac{d\sigma}{dt}$ for these reactions at $|t|>1$GeV[xx], - see fig.7c). If this observation will be confirmed by measurements of $d\sigma_{np}/dt$ at higher energies it will change the usual view, that the behaviour of $d\sigma_{NN}/dt$ in this t-range is determined by the exchange of the states with $I_t = 0$ only.

The results of the new measurements of the elastic pp-scattering at ISR in the large $|t|$ region are submitted to this Conference by CHOV group[19]. The data are obtained at $\sqrt{s} = 53$ GeV and up to $|t| \approx 9$ GeV^2, - fig. 8. The cross section has the well known minimum at $t=-(1.34\pm$

---

x/ Other types of parametrization were also used.

xx/ At lower energies $d\sigma/dt$ of np-and pp-scattering are equal within errors.

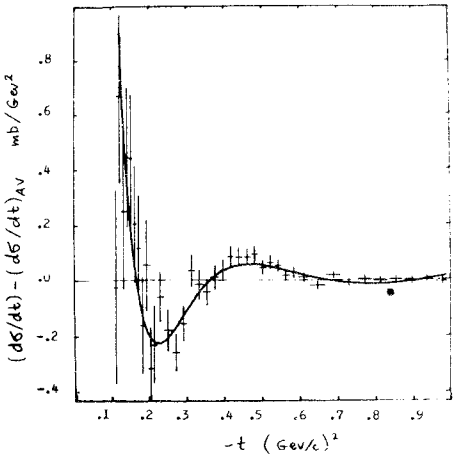

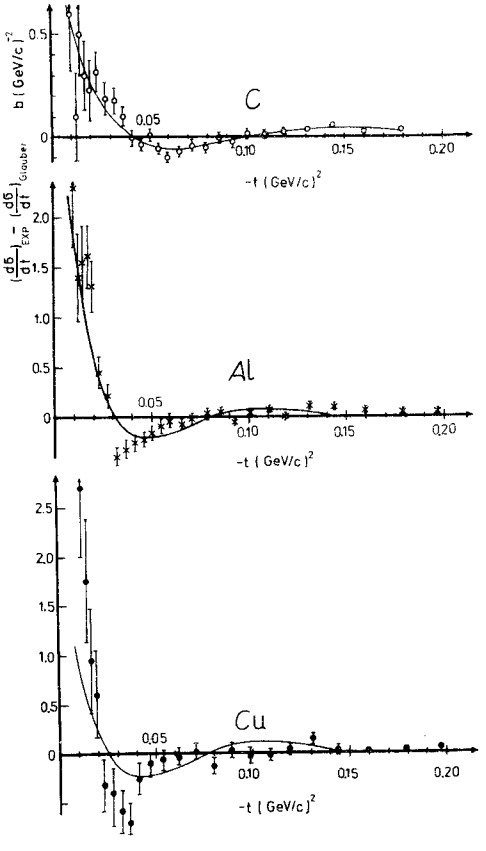

Fig. 6. The value of $d\sigma/dt - (d\sigma/dt)_{fit}$ a) in the elastic pp-scattering at 60 GeV/c[17], b),c) and d) in αA elastic scattering at 18 GeV/c[23]. Theoretical curves are from ref.[24].

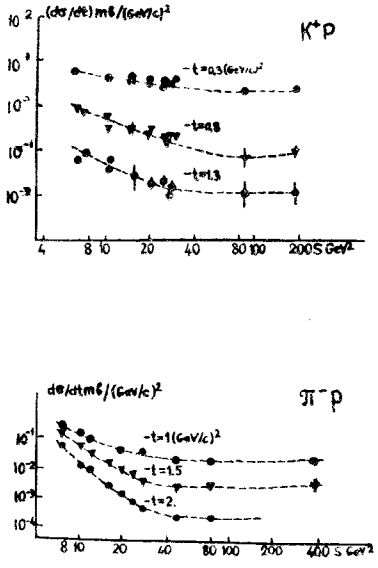

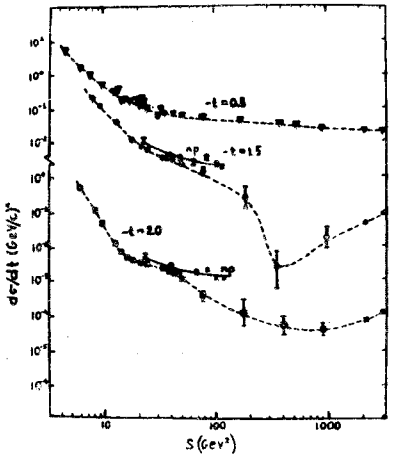

Fig. 7. Energy dependence of $\pi^- p$, $K^+ p$ and pp elastic scattering at fixed values of t. Figure taken from ref.[16], np-data[15,25]. The curves are drawn to guide the eye.

$\pm 0.02)\,\mathrm{GeV}^2$, but no further minimum or change of slope is observed between 2 and 6.5 GeV^2. This result rules out a number of theoretical models, which predict the minimum of $d\sigma/dt$ in this t-range.

Spin effects in the elastic NN-scattering (and quasi two-body processes) have been studied recently in Argonne[26-29] using polarized proton

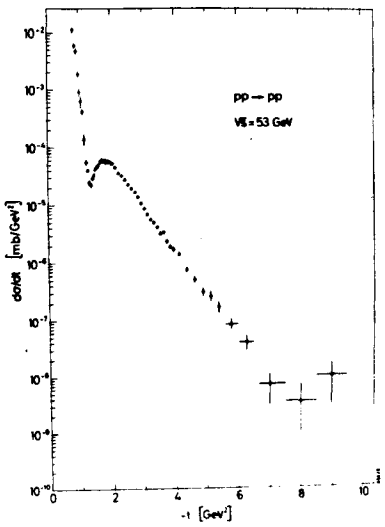

Fig. 8. Differential cross section of elastic pp -scattering at large t and $\sqrt{s} = 53$ GeV. Figure taken from ref./19/.

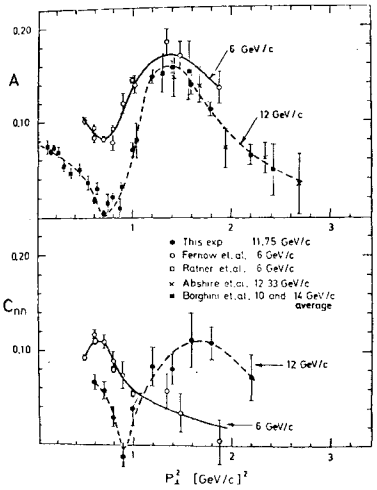

Fig. 9. Parameters A and C_{nn} for pp -elastic scattering. The curves are lines to guide the eye. Figure taken from ref./26/.

beam. The differential cross sections of the elastic pp-scattering in different spin states are measured up to an energy 11.75 GeV and the spin correlation parameter C_{nn} is determined, fig. 9. It is interesting, that in the region $|t| > 1$ GeV^2 spin effects are rather large and the parameter C_{nn} has peculiar energy dependence, - it decreases with s at $|t| < 1$ GeV^2 and increases at $|t| > 1$ GeV^2. Polarization in this last region has weak energy dependence. These phenomena are not yet explained theoretically and indicate also that the structure of NN-scattering in large $|t|$ region is more complicated, than it was previously believed.

IV. Theoretical Models

Theoretical models, used for the description of binary reactions, are based usually either on t-channel picture of the process, - the exchange in t-channel by the states with definite quantum numbers (Regge poles), or s-channel picture, - geometrical properties of the scattering or s-channel unitarity. This separation on t-channel and s-channel approaches is certainly rather arbitrary. In fact the models, which combine the features of both approaches are usually the most successful in the description of experiment. One of such examples is the absorptive Regge model/29-34/, where absorptive rescatterings in s-channel are applied to the Regge pole exchange in t-channel. The resulting amplitudes in this model have many properties, which are typical for "geometrical" models/34,35/.

The nature of Pomeranchuk singularity is the main problem for all theoretical approaches.

a) The parametrizations of elastic amplitudes.

The various phenomenological parametrization of amplitudes/34,36-38/ have been proposed for the description of elastic scattering at high energies. In the model/34/, for example, the following parametrization is used

$$T(s,t) = is\left[R_c^2 A_c e^{a_c t} \frac{J_1(R_c\sqrt{-t})}{R_c\sqrt{-t}} + R_e^2 A_e e^{B_e t} J_0(R_e\sqrt{-t})\right] \quad (2)$$

where $R_c^2 = R_{c0}^2 + R_{c1}^2(\ln s - i\pi/2)$, $R_e^2 = R_{e0}^2 + R_{e1}^2(\ln s - i\pi/2)$.

The first term in formula (2) corresponds to the "central" part of the amplitude (in the impact parameter space), and the second term to the "peripheral" or "edge" part. This parametrization gives good description of elastic processes at high energies/34/. The peripheral part in formula (2) is usually connected with the contribution of inelastic diffraction. Its

interference with central part leads to the change of slopes with t and it's square, - to the small oscillations of $d\sigma/dt$ [24]. The simple parametrization of amplitudes, which asymptotically leads to Froissart behaviour, is proposed in papers[36]. The model predicts negative value of the polarization in pp-scattering at energies larger than 200 GeV.

The assumption that Pomeron is the double pole was used for the description of elastic pp-scattering in the framework of dual approach[37,38].

Let us note that the different parametrizations of amplitudes, which differ strongly at $s\to\infty$ give a reasonable description of available experimental data on total cross sections, differential cross sections and polarizations of elastic scattering.

b) Regge Theory.

The Gribov's reggeon graphs theory[39] is the most successive approach to the problem of Pomeranchuk singularity. It gives the possibility to consider from unified point of view both binary and multiparticle processes. The question of intercept of "bare" Pomeranchuk pole $\alpha_0^P(0)$ is very significant for Regge theory. If the value of $\Delta\equiv\alpha_0^P(0)-1$ is equal to $\Delta_{crit}=\frac{\gamma_{PPP}^2}{4\alpha'_P}\ln\frac{4\alpha'_P}{\gamma_{PPP}^2}$ where γ_{PPP} is the triple Pomeron vertex, then the selfconsistent solution at $s\to\infty$ exists[40,41]. The variants of the theory with $\Delta>\Delta_{crit}$ were investigated recently[42,43]. The interest to the case $\Delta>\Delta_{crit}$ is connected mainly with two reasons: i) there are no arguments for $\alpha_0^P(0)$ to be exactly at the critical value, ii) present estimates of the $\gamma_{PPP}(0)$ from triple-Regge analysis of inclusive spectra give for Δ_{crit} the value $\approx 10^{-2}$. This shift of the bare pole is too small to explain the observed rise of the total cross sections in the framework of standard[x] approach[44]. But for $\Delta\approx 0.1$ it is possible to obtain a good description of the experimental data on the total cross sections and elastic processes in the diffractive cone region[43,44,46,47].

The hypothesis that the intercept of the Pomeranchuk pole is larger than unity and that it's eikonalization leads asymptotically to Froissart behaviour of scattering amplitudes was proposed several years ago by Cheng and Wu[48]. The most difficult problem for this approach is the question of consistency of the solution with it's iterations in t-channel and with t-channel unitarity. The first steps to the solution of this problem were made in papers[43], where the general set of reggeon graphs (fig. 10), which includes n to m Pomeron transitions, was considered under the assumption of analyticity in n,m first used by Cardy[49].

The input element in such approach is the amplitude of Fig. 10a), which corresponds to the iterations of Pomeranchuk pole in s-channel. It was shown, that the resulting system of equations

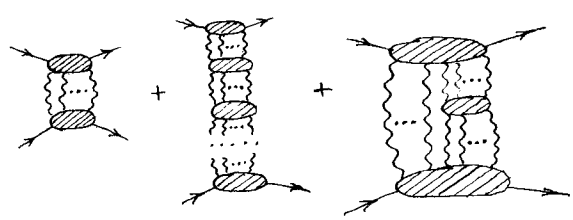

Fig. 10. Reggeon graphs considered in ref.[43].

has the selfconsistent solution (under some restrictions on the parameters of the theory), corresponding as $s\to\infty$ to the Froissart type behaviour of scattering amplitudes, - scattering on a black (or grey) disc with the radius $R\sim\ln s$. The asymptotic behaviour of scattering amplitudes in the framework of reggeon field theory with $\Delta>\Delta_{crit}$ and triple Pomeron interaction was investigated in ref.[42]. The solution again corresponds to the Froissart asymptotical regime. So it is natural to suggest that this regime is typical for a large class of Reggeon models with $\Delta>\Delta_{crit}$.

x/ In the framework of reggeon diagram approach the asymptotic formulae, which do not take into account a number of "threshold" effects, are usually used. It was shown in ref.[45], that it is possible to explain the rise of the total cross sections even in the case $\Delta=\Delta_{crit}$ taking into account these effects.

If one takes into account eikonal diagrams with the Pomeranchuk pole above one, then the elastic scattering amplitude has the well known form

$$T(s,t) = 8\pi s \int \frac{e^{2i\delta_R(s,b)} - 1}{2i} e^{i\vec{q}\vec{b}} \frac{d^2b}{2\pi} , \qquad (3)$$

$$\delta_R(s,b) = \frac{g_P(0)\,\gamma(\alpha_P(0))\,(s/s_0)^{\Delta}}{16\pi R^2(s)} \exp\left(-\frac{b^2}{4R^2(s)}\right) , \qquad (4)$$

where $\gamma(\alpha_P(0)) = \frac{1+e^{-i\pi\alpha_P(0)}}{\sin \pi\alpha_P(0)}$, $R^2(s) = R_0^2 + \alpha_P'(0)(\ln s/s_0 - i\pi/2)$.

In contrast to the parametrization, proposed in ref.[48], the slope of Pomeranchuk trajectory α_P' is taken into account in formula (4). Because of this the value of $\delta_R(s,0) \approx iC(1+\Delta \ln \frac{s}{s_0})/(1+\frac{\alpha_P'(0)}{R_0^2}\ln\frac{s}{s_0})$ practically does not depend on energy ($\Delta \approx \alpha_P'(0)/R_0^2$) at available energies[43] and the approximate geometrical scaling[50] takes place.

c) Geometrical Models.

The geometrical and optical models were extensively investigated in recent years. After the successful application of the hypothesis of geometrical scaling to pp-scattering at ISR energies[50] it was used for the description of other processes[51-55]. This hypothesis was generalized in order to take into account secondary exchanges[52,54,55] and real parts of amplitudes[55].

The ratios $\sigma^{(el)}(s)/\sigma^{(tot)}(s)$ and $b(s)/\sigma^{(tot)}(s)$ are different for πp, Kp and pp scattering. So it is clear that not only radii, but also opacities are different in these reactions. It was shown[52,55] that the best agreement with experiment was achieved, if the function $\delta(b/R(s))$ (not $f(b/R(s))$ or $G_{in}(b/R(s))$), obtained from pp-scattering, was multiplied by the constant factor dependent on the reaction - see fig. 11.

The ratios $b(s)/\sigma^{(tot)}(s)$ for particle and antiparticle scattering are very close (fig. 12). So it was supposed in papers[35,52,55] that the whole difference between the reactions of elastic AB and $\bar{A}B$ scattering is related to the difference of interaction radii. In the framework of such models the amplitudes of secondary exchanges (ρ,ω) in impact parameter (b) space are closely related to the b-space distribution

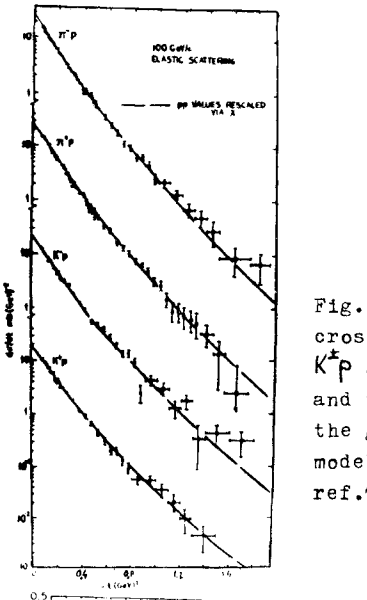

Fig. 11. Differential cross sections of $\pi^{\pm}p$, $K^{\pm}p$ scattering at 100 GeV and their description in the geometrical scaling model. Figure taken from ref.[50].

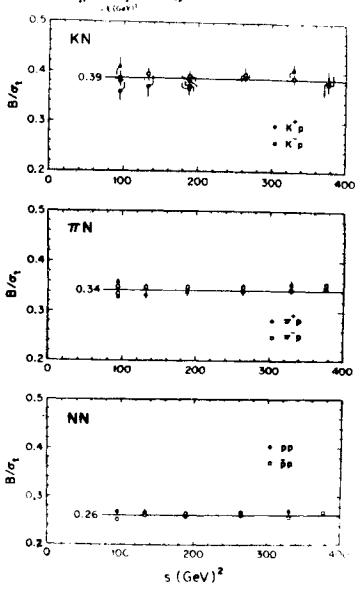

Fig. 12. Ratios $b(s)/\sigma^{(tot)}(s)$ for different elastic processes. Figure taken from ref.[50].

of the main (Pomeron) term and have the peripheral shapes[54,55]. As the functions $R_{AB(\bar{A}B)}$ depend on s, then due to the analyticity and crossing they have to contain some small imaginary parts. This approach gives a good description of elastic processes in a large energy range with a small number of free parameters[55]. In the framework of this model the differential cross section of elastic pp-scattering at the point of the minimum is proportional to the square of the real part of the amplitude at $t = 0$[55]

$$\frac{d\sigma/dt|_{t=t_{min}}}{d\sigma/dt|_{t=0}} \sim \frac{\rho^2}{1+\rho^2} . \qquad (5)$$

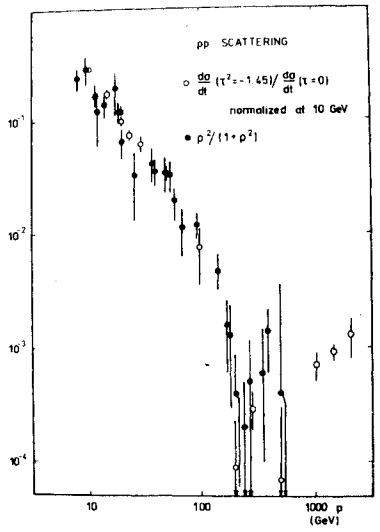

Fig. 13. The relation between $d\sigma_{pp}/dt|_{t=t_{min}}$ and $\varrho^2/(1+\varrho^2)$. Figure taken from ref./55/.

This relation agrees with experimental data (fig. 13) and relates the very pronounced dip in $d\sigma_{pp}/dt$ observed at $E_L = 200$ GeV/10/ with vanishing of ϱ in the same energy range.

The hypothesis of "b-universality" in the framework of geometrical approach leads to a simple systematics of helicity amplitudes/56,57/. The model, based on the b-universality and Regge approach, - "Reggeometry"/56/ describes successfully large class of two body processes, including meson-baryon backward scattering.

The assumption of the peripheral character of b-space distributions and of b-universality was used also for the description of inelastic diffractive processes/58-60/. The characteristic structures in t-distributions of the diffraction dissociation of nucleon (see below) actually point out to the peripheral character of these reactions. The account of absorption in the framework of Regge model for inelastic diffractive processes also leads to the peripheral b-space distributions/61,62/ (though b-universality is not valid in this model).

V. Inelastic Binary Reactions

The charge exchange reactions $\pi^-p\to\pi^0n$, $\pi^-p\to\eta n$, $\pi^-p\to\eta' n$ provide the most detailed information on the properties of the secondary (ϱ and A_2) exchanges.

The reactions $\pi^-p\to\eta n$ and $\pi^-p\to\eta' n$ [x] were studied recently in a large energy interval/63-67/ The following characteristic features of these processes are established:

a) There is a pronounced minimum in the $d\sigma/dt$ of $\pi^-p\to\eta^0 n$ at $t\to 0$, which points out to the dominant role of the spin-flip amplitude. The minimum is practically absent in the reaction $\pi^-p\to\eta' n$ /65/.

b) The effective A_2-trajectory is well determined and up to $|t|\sim 1$ GeV^2 is described by the straight line $\alpha^{eff}_{A_2}(t) = (0.426\pm0.007) + (.737\pm0.026)t$ /64/. A_2-intercept is certainly lower, than $\alpha^{eff}_{\varrho}(0)$. There is an indication to the strong curvature in A_2-trajectory at $|t|\gtrsim 1$ GeV^2.

c) There is a break at $|t|\sim 1.2$ GeV^2 in the t-dependence of the reaction $\pi^-p\to\eta^0 n$ - fig. 14 (the result is obtained in the high statistics experiment at Serpukhov at 40 GeV/c/66/). It is interesting to note, that the slope of $d\sigma/dt$ in

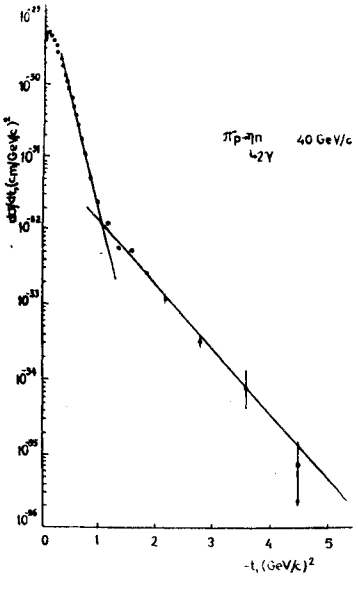

Fig. 14. Differential cross section of the reaction $\pi^-p\to\eta^0 n$ at 40 GeV/66/.

large $|t|$-region is close to one of pp-elastic scattering in the same $|t|$-range (see Sect. III), so both the phenomena may be of the same nature.

---

[x] The final results of the study of the reaction $\pi^-p\to\pi^0 n$ at FNAL energy range are discussed in the talk of A.V.Tollestrup at this Conference/63/.

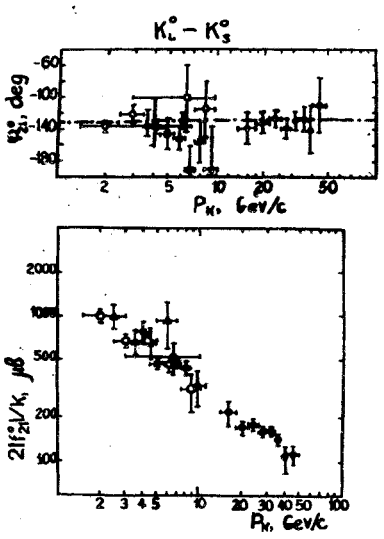

Fig. 15. Energy dependence of the phase and modulus of the amplitude of K_L^0-K_S^0 regeneration. The curve is the prediction of the model[70]. Figure taken from ref.[68].

The final results on the K_L^0-K_S^0 -regeneration on hydrogen and deuterium in the energy interval 10-50 GeV/c[68,69] show, that the modulus of the amplitude $|f_{21}|/K$ decreases with energy as $p^{-0.50\pm0.15}$ (for protons) and the phase is practically energy independent and is equal to $\varphi_{21} = -132\pm5^\circ$, - see fig.15. So these results are in agreement with Pomeranchuk theorem and the predictions of the models, which take into account ω, ϱ -poles and associated Regge cuts[70]. The differences of the total cross sections of $(\bar{K}^0p - K^0p)$ interaction and $(\bar{K}^0d - K^0d)$, determined from these experiments are in good agreement with the results of the measurements $\left(\sigma^{(tot)}_{K^-n} - \sigma^{(tot)}_{K^+n}\right)$ and $\left(\sigma^{(tot)}_{K^-d} - \sigma^{(tot)}_{K^+d}\right)$.

New interesting results on the nucleon charge exchange reactions $pn \to np$ and $\bar{p}p \to \bar{n}n$ at high energies have been obtained in the past two years[71-74]. The investigations of the reaction $pn \to np$ at $p_L \lesssim 30$ GeV/c showed, that $d\sigma/dt \sim 1/p_L^2$ and $\alpha_{eff}(t) \approx 0$ in the region $|t| < 1$ GeV^2. This result can be connected with the dominant role of the π-Regge pole and (πP)-cut at small t, while ϱ and A_2-exchanges are important at larger $|t|$ values. The models[34,75] predict the change in the energy behaviour at $p_L > 30$ GeV, due to the gradual increase with energy of the relative weight of ϱ and A_2-contributions.

This qualitative prediction of Regge approach is confirmed by the recent experimental data from Serpukhov[71] and FNAL[72], - at highest energies ($p_L \gtrsim 100$ GeV) and small $|t|$ $d\sigma/dt \sim 1/p_L$ $(\alpha_{eff} \approx 0.5)$. The quantitative agreement of the data with the predictions of the models[34,75] can hardly be considered as satisfactory[76].

Sharp minimum at $t = -\mu_\pi^2$ in the differential cross section of the reaction $\bar{p}p \to \bar{n}n$ has been found previously at energy 40 GeV[73]. The existence of the dip is confirmed by the new data of the same group at 30 GeV[74] - fig. 16.

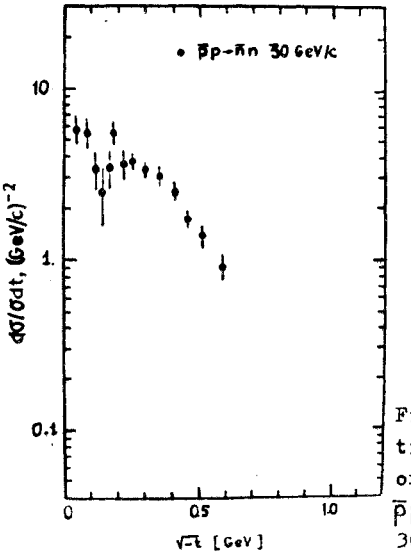

Fig. 16. Differential cross section of the reaction $\bar{p}p \to \bar{n}n$ at 30 GeV[74].

Theoretical models, mentioned above predict the minimum in $d\sigma/dt$ at $t = -\mu_\pi^2$, but its depth and the form of $d\sigma/dt$ at small $|t|$ do not agree with the experimental data. It was pointed out in ref.[77], that this disagreement may lead to the important consequences for the theoretical approaches to the binary reactions. Further investigations of this question are needed.

The number of interesting investigations of quasi-two-body reactions is submitted to this Conference[78-95]. The detailed study of the polarizations and spin-density matrices of the produced particles and resonances and careful amplitude analysis of some reactions revealed many interesting properties of these processes. I'll briefly discuss some of them.

a) Parameters of the effective Regge-trajectories are universal, i.e., they do not depend

on the processes, from which they were determined. For example effective ϱ-trajectory, found from the reaction $\pi^+p \to \pi^0\Delta^{++}(1236)$ and ϱ-A_2 -trajectory from $\pi^+p \to \eta\Delta^{++}(1236)$ and $K^+p \to K^0\Delta^{++}(1236)$ are in good agreement with the values, found in $\pi^-p \to \pi^0 n$, $\pi^-p \to \eta n$ - fig. 17.

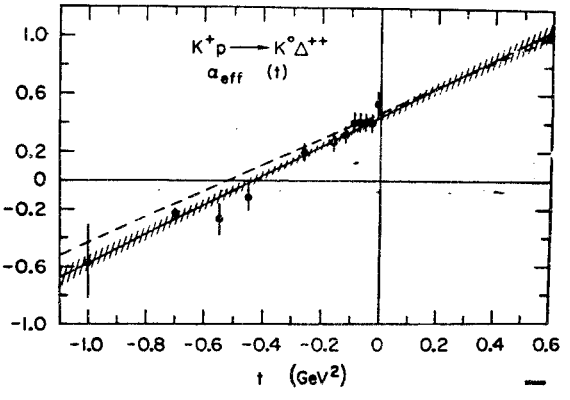

Fig. 17. Effective ϱ-A_2 -trajectory from the reaction $K^+p \to K^0\Delta^{++}$. Figure taken from ref./80/.

b) Pion Regge pole is a dominant exchange (in the reactions where it is allowed by quantum numbers) in the region of small $|t| \lesssim 0.2$ GeV^2 and intermediate energies $E \lesssim 30$ GeV. It, probably, has the same slope (~ 1 GeV^{-2}) as the other Regge-trajectories/96,97,81,95/. Amplitude analysis of the reactions $K^-p \to (K^-\pi^+)n$, $K^+p \to (K^+\pi^-)\Delta^{++}$ /81/ and $\pi^+p \to (\pi^+\pi^-)\Delta^{++}$ /91/ shows, that the contributions of the states with "natural" quantum numbers in t-channel (ϱ, A_2) are important at $|t| \gtrsim 0.3$ GeV^2 for the production of resonances with small masses ($K^*(890)$, ϱ). As the mass of the produced system increases the relative weight of these contributions as well as of $(\pi\varrho)$-cut decreases.

The first data on the quasi two-body (non-diffractive) reaction $pp \to n\Delta^{++}$ at ISR energies are submitted to this Conference by CHOV-group/93/. It decreases rapidly with energy (as $1/p^{1.94\pm0.03}$ up to $\sqrt{s} = 23$ GeV) in agreement with the dominant contribution of π-exchange. There is an indication to the slower decrease with S at highest energies. This is, possibly, connected with manifestation of ϱ , A_2-exchanges.

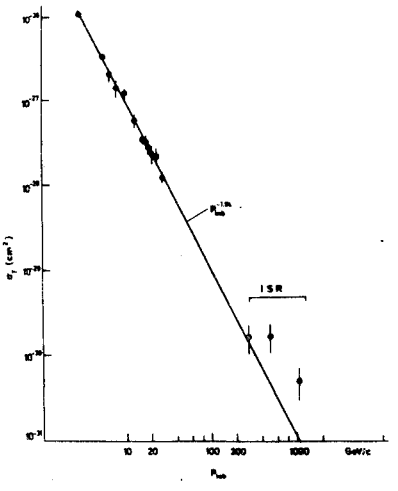

Fig. 18. The cross section of the reaction $pp \to n\Delta^{++}$ as a function of energy. Figure taken from ref./93/.

c) The existence of the exchanges with quantum numbers $\sigma P = -1$, $\sigma G(-1)^I = +1$ (σ -signature) was clearly demonstrated in high statistics experiments, - study of $\pi^-p \to \omega n$ at 6 GeV/88/ and $\pi^-p \to \varrho^0 n$ on a polarized target at 17 GeV/94/. The question of the existence of such trajectories ($\mathcal{X}$ with $\sigma = +, P = -, G = +, I = 1$/98/ and A_1 with $\sigma = -$, $P = +$, $G = -$, $I = 1$) is of importance for classification of particles and resonances. These results can be also explained in terms of Regge-cuts (πA_2, $\pi\varrho$)/99/. The investigation of the energy dependence of these effects is needed to clarify the situation.

d) The predictions of the hypothesis of strong exchange degeneracy (SED) or dual diagrams are often in a clear contradiction with experimental data/83,84/ (see also/57/). For example polarizations in the reactions $\pi^+p \to K^+\Sigma^+$, $K^-p \to \pi^-\Sigma^+$/87/ which should be equal to zero, if SED is valid, reach the maximum values $|P| \approx 1$.

e) The predictions of simple additive quark model are usually in a reasonable agreement with experimental data/83,85,90/. (The deviations from quark model predictions are seen in some cases. For example in the decay angular distribution of Δ^{++} in the reaction $K^+p \to K^0\Delta^{++}$/85/ in region of small $|t|$).

VI. Inelastic Diffractive Processes

In recent years our knowledge of inelastic diffraction was greatly improved[x] due to considerable extension of the energy range, accessible for experimental investigation and high accuracy of the data.

1). Exclusive diffractive reactions

The results of the investigation of a number of exclusive reactions with small number of particles in final states, - $NN \to N(N\pi)$ /101-105/, $\pi N \to \pi(N\pi)$ /106-108/, $K^-p \to K^-(n\pi^+)$ /113/, $\pi^+p \to \pi^+\pi^+\pi^-p$ /109/, $pp \to pp\pi^+\pi^-$/110,111/, $\bar{p}p \to \bar{p}p\pi^+\pi^-$ /112/, $K^\pm p \to K^\pm\pi^+\pi^-p$ /113-116/ give rather complete picture of the properties of diffraction dissociation:

a) Weak energy dependence (see for example fig 19).

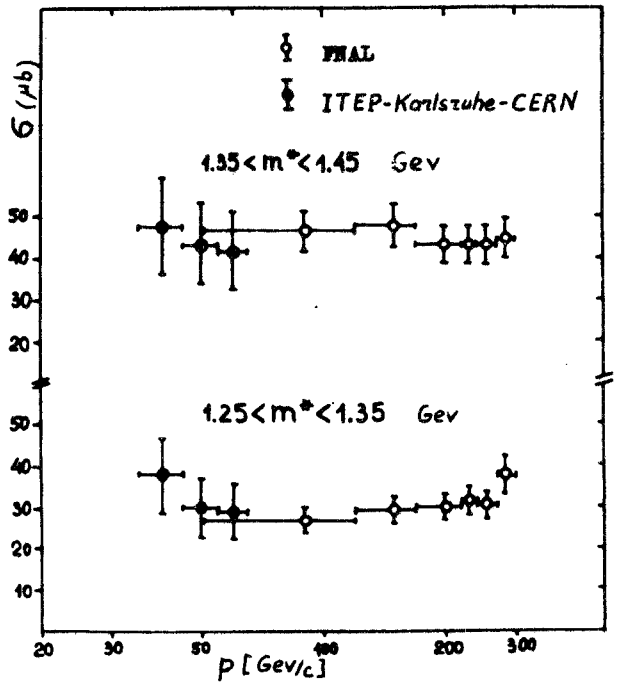

Fig. 19. Energy dependence of $d^2\sigma/dM^2dt$ of the reaction $np \to (p\pi^-)p$ /102,103/.

It is very interesting to study, whether there is a rise of $d\sigma/dM^2dt|_{t=0}$ with energy, as predicted by some theoretical models/43,48/ which describe the increase of $\sigma^{(tot)}$ (Let us note, that the increase of $d\sigma/dt$ for inelastic diffraction can happen even at higher energies, than for elastic scattering. The early rise is expected to be in the reaction $K^+p \to K^+(n\pi^+)$).

b) The mass-spectra of diffractively produced systems are concentrated in a region of rather small masses ($M \lesssim 2$ GeV). Their form depends weakly on initial energy and the type of colliding particles (see fig. 20). In the threshold region of $N\pi$-system ($M \lesssim 1.4$ GeV) the forms of the mass-spectra are determined mainly by the Drell-Hiida-Deek (DHD)-type diagrams - fig. 21a)-c) (see papers/119-123/ and the talk by L.A.Ponomarev/118/). At higher masses the contributions of resonances at M = 1.5, 1.68 and (possibly) at 2.1 GeV/c are important/101-108,113,117/. Approximate factorization takes place.

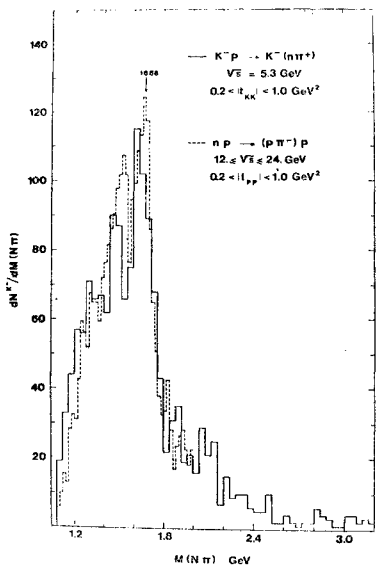

Fig. 20. The comparison of $N\pi$ - mass distributions in $K^-p \to K^-n\pi^+$/113/ and $np \to (p\pi^-)p$/103/. Figure taken from ref./113/

c) The momentum transfer t distributions depend strongly on mass of the produced system (slope-mass correlations). The strong dependence of the slope on the polar angle $\cos\theta_J$ (in the Gottfried-Jackson system) of the diffractively produced nucleon in the reaction $NN \to (N\pi)N$ - see fig. 22, - was discussed recently/95-97,101,112/. These correlations are partly explained by the pion exchange diagram of fig. 21a) (dashed curves in fig. 22), but much better agreement with experiment is obtained if all the diagrams

---

[x] Detailed discussion of some questions of the diffraction dissociation, which will be only shortly mentioned in my report, can be found in a number of reviews on this subject/100/.

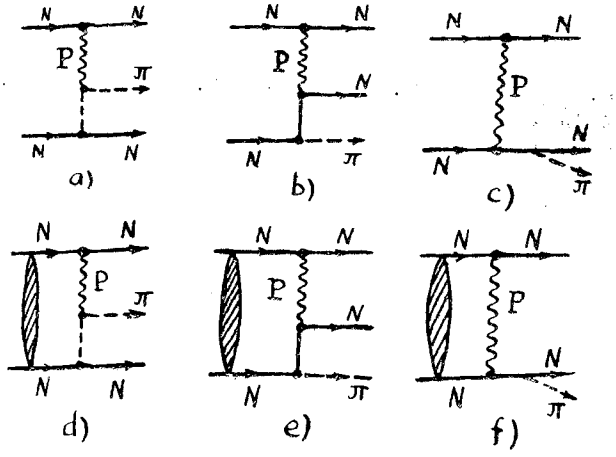

Fig. 21. The diagrams of DHD-model, -a)-c), and absorptive corrections to them -d)-f).

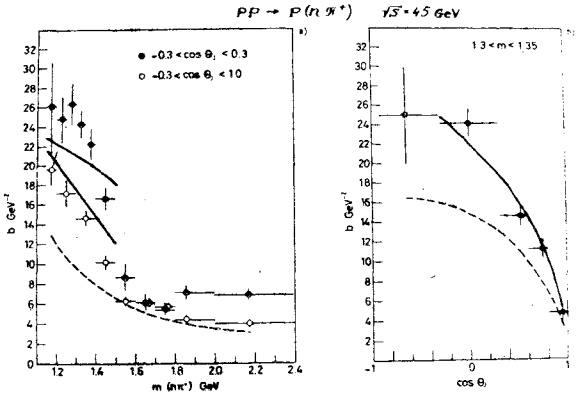

Fig. 22. The dependence of the slope b in the reaction $pp \to p(n\pi^+)$ on $M_{n\pi^+}$ and $\cos\theta_j$ /101/. The dashed curves are the results of calculations in pion Deck model. - fig. 21a). The full curves are obtained with the account of the other graphs of fig. 21 (see ref./118/).

of fig. 21 are taken into account (full curves in fig. 22/118/).

In the region of small masses of $N\pi$ and $N\pi\pi$ - systems there are dips and breaks in t-distributions. These structures depend both on mass and $\cos\theta_j$ /101,103,117/, - see for example fig.23. The dip is the most clearly seen in the region $M < 1.35$ GeV and $\cos\theta_j \approx 0$. In the framework of DHD-model such t-dependence can be reproduced only if the absorptive corrections fig.21d)-f) to the diagrams of fig. 21a)-c) are considered/118/. The structures in t-distributions

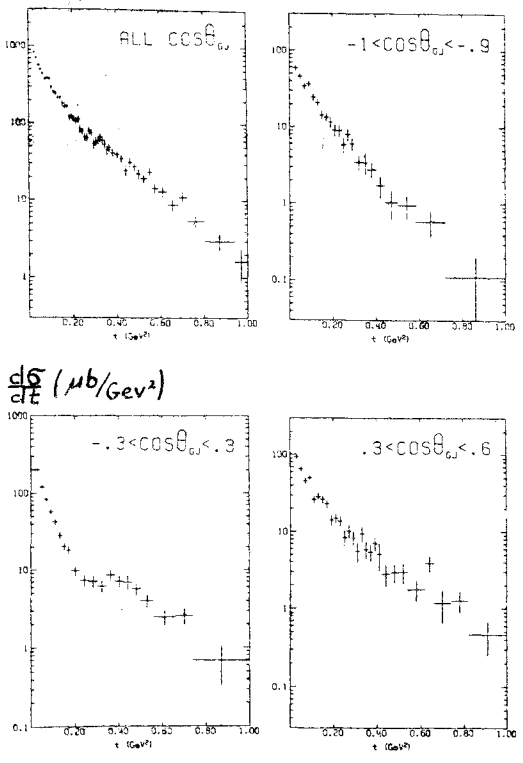

1.35 < M < 1.55

Fig. 23. The $d\sigma/dt$ in the reaction $np \to (p\pi^-)p$ for $1.35 < M_{p\pi^-} < 1.55$ GeV and different intervals of $\cos\theta_j$ /103/.

under the diffractive dissociation of nucleon are usually interpreted as a manifestation of a peripheral character of the amplitudes of inelastic diffraction in impact parameter space. But it should be noted, that there is no evidence for such a structure in the diffraction dissociation of K-mesons in the reaction $Kp \to (K\pi\pi)p$ /113/. The amplitude analysis of $(K\pi\pi)$ system/114/ shows, that there are slope-mass correlation for the diffractively produced states with given quantum numbers. These results contradict to the hypothesis of b-universality for diffractive reactions.

d) The backward peak in $\cos\theta_j$ distributions is observed in the reactions $NN \to (N\pi)N$ at high energies/101-103,117/ - fig. 24. The fact, that the peak is seen also in the region of small masses of $N\pi$-system ($M_{N\pi} < 1.4$ GeV), where the contribution of resonances is small, indicates to the important role of the nucleon exchange (fig. 21b) in the amplitudes of the

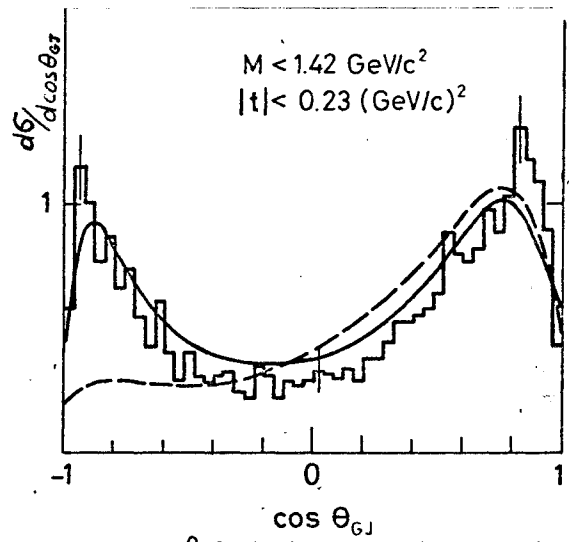

Fig. 24. The $\cos\theta_J$ distribution in the reaction $np\to(p\pi^-)p$ at 60 GeV and $M_{p\pi^-}<1.35$ GeV /102/.

diffraction dissociation of nucleon. The theoretical analysis of these reactions in the framework of DHD-model /118-123/ shows that not only t- and u-channel diagrams of fig. 21a), b) but also s-channel graph, - fig. 21c) should be taken into account in order to describe the main features of the experimental data.

e) It follows from the investigations of the azimuthal angular distributions that in the inelastic diffractive processes in general the helicity is not conserved neither in t- nor in s-channel. The DHD-models reproduce the main trends of the φ-dependence /118/.

f) The Morrison rule is violated. The amplitude analysis of the reaction $\pi N\to\pi(\pi N)$ at 16 GeV/c /106/ has shown that at low masses of πN -system the $J^P=1/2^-$ (s-wave) is diffractively produced[x/].

All these results demonstrate that the exclusive diffractive processes have very rich and interesting structure. Theoretical understanding of the correlation effects, seen in experiment, is far from being complete. The best results are obtained in the framework of DHD-model which takes into account a coherent sum of all the diagrams of fig. 21 with proper spin dependence.

3. Inclusive Diffractive Processes

The inclusive diffractive production of hadrons at high energies was investigated in past few years by many experimental groups /124-135/. The interest to these reactions is connected mainly with the discovery of the diffractive production of the high mass hadronic systems. This phenomenon is usually interpreted in terms of triple-Pomeron interaction. The phenomenological analysis allows to determine the effective triple-Pomeron coupling /136-142/, which is important for the Regge approach to high energy scattering.

I shall briefly discuss some properties of inclusive processes at high energies in the diffractive region $(M^2/s\ll 1)$.

a) The invariant inclusive cross section $\rho=Ed^3\sigma/d^3p$ of the reaction $pp\to pX$ does not depend on energy s at fixed value of x $(1-x\approx M^2/s)$ at $s>500$ GeV^2 /124/ - so within the errors of 5 - 10% scaling takes place. In the region of small $|t|$ and $x\to 1$ the spectra have pronounced peak, which is consistent with the behaviour $\rho\sim\frac{1}{1-x}$ (see fig. 25), expected for the triple-Pomeron interaction.

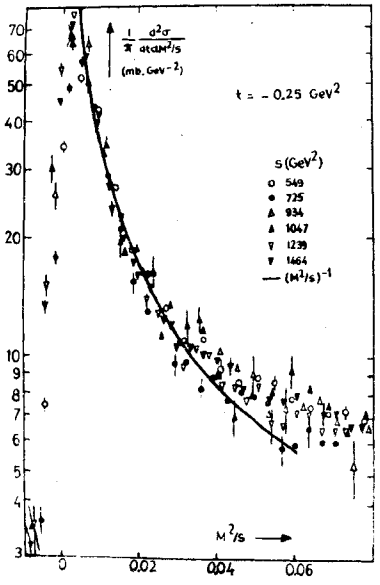

Fig. 25. The function $\rho=Ed^3\sigma/d^3p$ of the processes $pp\to pX$ at high energies. Figure taken from ref./124/.

[x/] The authors of ref./106/ used an interesting method of amplitude analysis, - the study of the interference between $I_t=0$ (diffractive) and $I_t=1$ (ρ) components in order to determine unambiguously the quantum numbers of πN-system.

b) In the region $1-x > 0.05$ there is a substantial contribution of the secondary exchanges, which leads to the slower decrease of ς as $(1-x)$ increases. New data on the reaction $pd \to Xd$ are obtained at ISR with the help of deuteron beam[126] and at FNAL[125]. The spectra in this reaction have the shape, which is very similar to the one in the process $pp \to Xp$, fig. 26. (The cross section of $pp \to pX$ in fig. 26 is

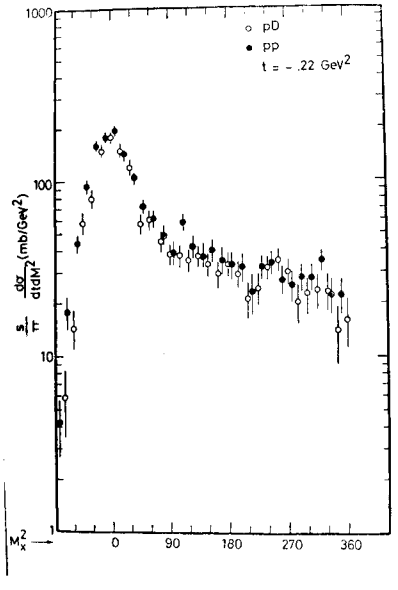

Fig. 26. The spectra in the reactions $pd \to Xd$ and $pp \to Xp$ at ISR[126].

scaled down by the measured ratio of the differential elastic cross sections). This observation can be interpreted[126] as the smallness of the contributions of exchanges with $I=1$ (which are absent in the case of the reaction $pd \to Xd$)[x].

c) The slope of t-distributions decreases with M^2 at $M^2 < 10$ GeV^2. In the region $M^2 \geq 10$ GeV^2 the slope practically does not depend on M.

d) The total cross section of inelastic diffraction σ_D rises with energy, because of the mass of the system, which can be produced diffractively, increases with S ($M^2 = \alpha S$, $\alpha \ll 1$). It is interesting to answer the question - whether the rise of σ_D can explain the rise of $\sigma_{inel}^{(tot)}$ in the ISR-energy range? The data

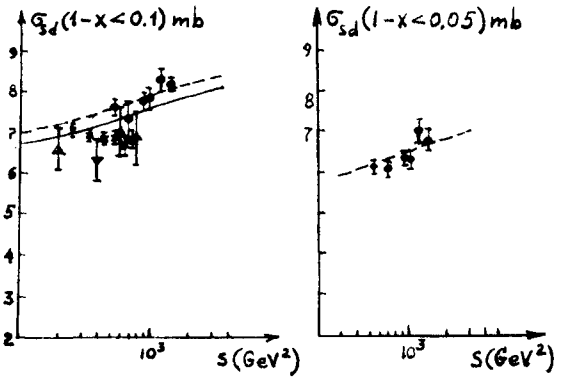

Fig. 27. The energy dependence of the cross section in the diffractive region. The curvature in t-dependence of high mass diffraction is taken into account in theoretical calculation (full curve), the same curvature is assumed to be present in low mass ($M^2 \leq 4$ GeV^2) -dashed curve.

on the energy dependence of the inclusive cross section of the process $pp \to Xp$ in the diffractive region[124] and theoretical calculations, based on the triple-Regge phenomenology, are shown in fig. 27. Both the theoretical calculation and experimental results show that the increase of σ_D in the ISR energy range is insufficient to explain all the rise of $\sigma_{inel}^{(tot)}$.

e) The processes of double diffraction excitation both in inclusive and exclusive channels were investigated recently[134,135,143,144]. These experiments demonstrated the validity of factorization in the region of $|t| < 0.5$ GeV^2. The most precise test of factorization in the double diffractive processes has been performed in ref.[135]. The reactions $pp \to pX$, $pp \to (p\pi^+\pi^-)X$ and $pp \to (\Lambda^0 K^+)X$ have been measured (X - can be either proton or some hadronic state) in the diffractive region ($1-x < 0.1$). If factorization is valid, then the ratios $R_i = \frac{d\sigma/dt(pp \to ip)}{d\sigma/dt(pp \to iX)}$ where $i = p, (p\pi^+\pi^-), (\Lambda^0 K^+)$ should be equal. It follows from fig. 28, that factorization takes place at $|t| < 0.5$. At larger values of $|t|$ there is apparent breakdown of factorization. It is interesting to note that in an agreement with factorization the mean slope of t-dependence in double dissociation processes is very small, $b = (2.2 \pm 0.2)$ GeV^{-2}[135].

[x] This statement should be taken with caution, because the spectra were compared at the same value of S, but it is more reasonable from theoretical point of view to compare the functions $d^2\sigma/dtdM^2$ at the same energy E_{LAB}.

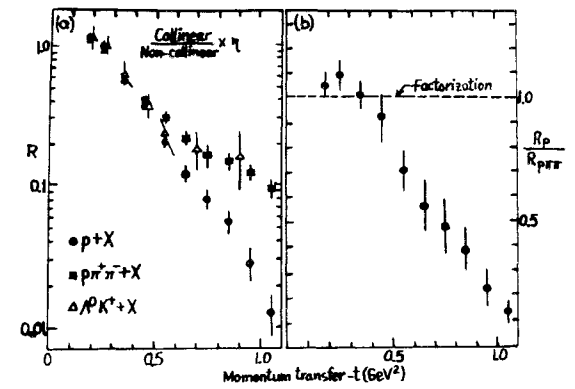

Fig. 28. Test of the factorization in the processes of double diffractive excitation. Figure taken from ref.[135].

3. Double Pomeron Exchange

The very high energies available now make possible the experimental investigation of a completely new class of diffractive processes, namely double Pomeron exchange reactions (DPE). The existence of DPE mechanism of particle production - fig. 29a) - is very natural from t-channel point of view. In the framework of Regge theory the cross section of inclusive processes $pp \to pXp$ in the DPE-region of phase space ($1-x_1, 1-x_2 \ll 1$; two large rapidity gaps, - fig. 29b)) is connected with the new quantity -

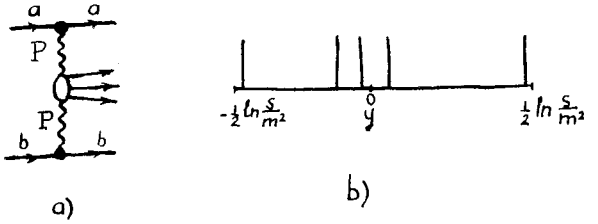

Fig. 29. a) The diagram of DPE, b) rapidity distribution of final particles, corresponding to DPE.

the total cross section of Pomeron-Pomeron interaction. The behaviour of PP-interaction (especially at small $|t_i|$ region) is of great importance for existing theoretical approaches to the scattering of hadrons at very high energies (see for example[145]).

The experimental information on the DPE[110,111,146-150] is still rather fragmentary.

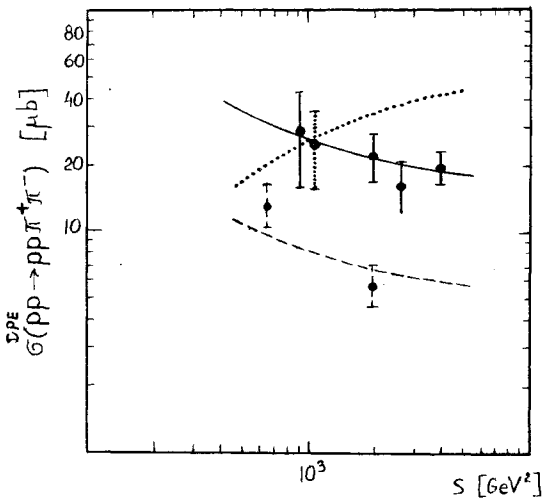

Fig. 30. The contribution of DPE to the cross section of the reaction $pp \to pp\pi^+\pi^-$. The theoretical calculation (full curves) take into account the "background" contribution and kinematical cuts of the experiments[145].

The cross sections of DPE reactions are very small. The results of the recent experiments, performed at ISR, on the study of DPE in the reaction $pp \to pp\pi^+\pi^-$ are shown in fig. 30. Theoretical calculations[145] are also shown in this figure. It follows from fig. 30 that: a) the absolute values of the cross sections, as well as their energy dependences, are strongly influenced by the experimental cuts, b) existing data are in an agreement with theoretical expectations. It should be noted that the "background" contribution, which is due to the "tail" of the single diffraction dissociation or in other words due to the secondary exchanges is important even in the conditions of the experiments at ISR-energies. The unambiguous evidence for DPE can result only from a detailed analysis of the energy dependence of the differential cross sections at fixed mass of the produced system[145]. More work in this direction is needed to establish reliably existence of DPE.

VII. Summary and Conclusions

1. The investigation of the total cross sections of hadronic interactions and elastic scattering at very high energies demonstrated

that the results, which follow from the basic properties of theory, dispersion relations and asymptotic theorems are in an agreement with experiment.

2. The change in the behaviour of $\sigma^{(tot)}$ and $\rho = Re T(s,0)/Im T(s,0)$ at $E \sim 100$ GeV points out that we are in a "threshold" of asymptotic region. Current theoretical models show, that the energies, where "true" asymptotic behaviour is valid, are much higher.

3. New effects are seen (probably) in elastic scattering:

a) The decrease of the pp-slope with t as $t \to 0$.

b) Small oscillations of $d\sigma/dt$ in the region of diffraction cone.

c) The increase of spin-spin correlations with energy.

d) Inequality of $d\sigma_{p\bar{p}}/dt$ and $d\sigma_{pp}/dt$ at $|t| > 1$ GeV^2 and $E_{Lab} > 30$ GeV.

e) There is only one pronounced dip (at $|t| \approx$ $\approx$ 1.3GeV^2) in $d\sigma/dt$ of pp-scattering at very high energy and $|t| < 6.5$ GeV^2.

4. The nature of Pomeranchuk singularity is the main problem for theoretical approaches to high energy scattering. The models with Froissart-type asymptotic behaviour of amplitudes are on the firmer theoretical basis now and can be considered as good candidates for the description of diffraction at $S \to \infty$. Due to smallness of the $\Delta = \alpha_P(0) - 1$ the Pomeranchuk pole is still the main contribution to amplitudes at present energies.

5. Effective Regge-trajectories for secondary exchanges are universal.

6. Geometrical approaches are useful in the phenomenological analysis of two-body reactions.

7. New level is achieved in the investigation of exclusive diffraction production of particles. Interesting correlations are observed. Theoretical models reproduce some characteristic features of the data.

8. Approximate factorization takes place in diffractive processes.

9. Double Pomeron exchange is the new phenomenon and its further investigation may give new insight into properties of diffraction.

Acknowledgements

I would like to thank K.G.Boreskov, Yu.Kamyshkov, V.A.Lyubimov, L.A.Ponomarev, Yu.D.Prokoshkin, K.A.Ter-Martirosyan, P.Shelein, V.A.Tsarev, A.B.Wicklund and N.P.Zotov for valuable discussions and K.G.Boreskov for help in preparing this report.

References

1. G.Belletini et al. Conference paper. No. 1157/A1-5.
2. U.Amaldi et al. Phys.Lett., 44B, 112 (1973). S.R.Amendolia et al. Phys.Lett., 44B, 119 (1973).
3. A.S.Carrol et al. Phys.Lett., 61B, 303 (1976).
4. S.P.Denisov et al. Phys.Lett., 36B, 415 (1971); 36B, 528 (1971); Nucl.Phys., 65B, 1 (1973).
5. V.D.Apokin et al. Conference paper No. 42/A1-42.
6. R.K.Carnegie et al. Phys.Lett., 59B, 308 (1975) and Conference paper No. 290/A1-105.
7. P.Jenni et al. Nucl.Phys., B94, 1 (1975). P.Baillon et al. Nucl.Phys., B105, 365 (1976). P.Baillon et al. CERN Preprint 76-1.
8. C.Ankenbrandt et al. FERMI LAB-Conf-75/61 EXP.
9. D.S.Ayres et al. Phys.Rev.Lett., 35m 1195 (1975).
10. C.W.Akerlof et al. Phys.Rev.Lett., 35, 1406 (1975).
11. C.Baglin et al. Nucl.Phys., B98, 365 (1975).
12. R.K.Carnegie et al. Phys.Lett., 59B, 313 (1975) and Conference paper No. 266/A1-120.
13. G.Brandenburg et al. Conference paper No. 267/A1-81.
14. R.K.Carnegie et al. Conference paper No. 721/A1-124.
15. V.Bohmer et al. Nucl.Phys., B91, 266 (1975).
16. K.Bruneton et al. Conference paper No. 817/A1-123.
17. Yu.M.Antipov et al. Conference paper No. 40/A1-40.
18. N.Kwak et al. Phys.Lett., 58B, 233 (1975).
19. H. de Kerret et al. Conference paper No. 75/A1-75.

20. C.Ankenbrandt et al. Conference paper No. 1242/A1- 167.
21. V.Bartenev et al. Phys.Rev.Lett., 31, 1088 (1973).
22. G.Barbiellini et al. Phys.Lett., B39, 663 (1972).
23. V.G.Ableev et al. Conference paper No. 448/A6-5.
24. N.I.Starkov, V.A.Tsarev. JETP Letters, 23, 403 (1976); and the Talk at this Conf.
25. J.Engler et al. Nucl.Phys., B62, 160 (1973).
26. K.Abe et al. Conference paper No.1209/A1-162.
27. A.B.Wicklund et al. Paper No. 61/A1-61. and invited talk at this Conference.
28. R.Diebold et al. Phys.Rev.Lett., 35, 632 (1975) and Conference paper No. 1153/A1-153.
29. R.C.Arnold. Phys.Rev., 153, 1523 (1967).
30. G.Cohen-Tannoudji, A.Morel, Ph.Salin. Nuovo Cim., 55A, 412 (1968).
31. F.S.Henvey, G.L.Kane, J.Pumplin, M.H.Ross. Phys.Rev., 182, 1579 (1969).
32. K.A.Ter-Martirosyan. Yad. Fiz., 10, 1047 (1969).
33. A.B.Kaidalov, B.M.Karnakov. Phys.Lett., 29B, 372, 376 (1969).
34. G.L.Kane and A.Seidl. Reviews of Modern Phys., 48, 309 (1976).
35. A.B.Kaidalov. Yad.Fiz., 16, 401 (1972).
36. L.D.Soloviev. JETP Letters, 18, 455 (1973); 19, 185 (1974).
L.D.Soloviev, A.V.Shchelkachev. Conference paper No. 45/A1-45.
37. A.I.Bugrij et al. Lett.Nuovo Cim., 6, 577 (1973) and A.I.Bugrij et al. Conference paper No. 14/A1-14.
38. A.N.Wall et al. Conference paper No. 17/A1-17.
39. V.N.Gribov. JETP, 53, 654 (1967).
40. A.A.Migdal, A.M.Polyakov, K.A.Ter-Martirosyan. Phys.Lett., 48B, 239 (1974); JETP, 67, 848 (1974).
41. H.D.I.Abarbanel, J.B.Bronzan. Phys.Lett., 48B, 345 (1974); Phys.Rev., D9, 2397 (1974).
42. D.Amati, L.Caneschi, R.Jengo. Nucl.Phys., B101, 397 (1975).
V.Allessandrini, D.Amati, R.Jengo. CERN Preprint TH.2089 (1975).
D.Amati et al. CERN Preprint TH.2152 (1976).
43. M.S.Dubovikov, K.A.Ter-Martirosyan. Preprint ITEP-37, Moscow (1976) and Conference paper No. 23/A1-23.
B.Z.Kopeliovich, L.I.Lapidus. JINR, E2-9537, Dubna (1976).
M.S.Dubovikov et al. Conference paper No. 814/A1-134.
44. A.Capella, J.Kaplan. Phys.Lett., 52B, 448 (1974). A.Capella, J.Kaplan and J.Tranh Thanh Van. Nucl.Phys., B97, 493 (1975).
45. A.Capella, A.Kaidalov. CERN Preprint TH.2151 (1976).
46. P.D.Collins et al. Phys.Lett., 47B, 171 (1973); Nucl.Phys., B80, 135 (1974); B83, 241 (1974).
47. P.E.Volkovitskii, A.M.Lapidus, K.A.Ter-Martirosyan. Conference paper No. 24/A1-24.
48. H.Cheng, T.T.Wu. Phys.Rev.Lett., 24, 1456 (1970).
H.Cheng, J.K.Walker, T.T.Wu. Phys.Lett., 44B, 97 (1973) and Conference paper No. 284/A1-116.
49. J.L.Cardy. Nucl.Phys., B75, 413 (1974).
50. J.Dias de Deus. Nucl.Phys., B59, 231 (1973).
A.J.Buras, J.Dias de Deus. Nucl.Phys., B71, 481 (1974).
51. W.Grein, P.Kroll. Phys.Lett., 58B, 79 (1975).
52. V.Barger, J.Luthe, R.J.N.Phillips. Nucl. Phys., B88, 237 (1975).
V.Barger, R.J.N.Phillips. Preprint RL-75-176 and Conference paper No. 310/A1-93.
53. J.Fröyland. Phys.Lett., 58B, 317 (1975); 60B, 87 (1975).
54. J.P.Ader, R.Peschanski and R.Lacaze. CERN Preprint TH 2112 (1976).
55. J.Dias de Deus, P.Kroll. Conference papers No. 388/A1-80, 389/A1-79.
56. J.P.Ader et al. Nuovo Cim., 27A, 385 (1975).
J.P.Ader, Nucl.Phys., B98, 154 (1975).
57. F.Schrempp, B.Schrempp. Rapporteur Talk at the International Conference on High Energy Physics, Palermo, CERN Preprint TH.2054.
58. G.L.Kane. Acta Phys.Polon., B3, 845 (1973).
59. N.Sakai, J.N.J.White. Nucl.Phys., B59, 511 (1973).
60. S.Humble. Nucl.Phys., B86, 285 (1975).
61. V.Tsarev. Phys.Rev., 11D, 1864, 1875 (1975).
62. E.L.Berger, P.Pirila. Preprint ANL-HEP-PR-75-27 (1975); and Conference paper No. 56/A1-56.
63. A.V.Barnes, D.J.Millema, A.V.Tollestrup et al. Conference paper No. 967/A1-128 and invited talk of A.V.Tollestrup at this Conference.
64. M.H.Shaevitz et al. Phys.Rev.Lett., 60B, 117 (1975) and Conference paper No. 405/A1-99.
65. K.W.Edwards et al. Conference paper No. 403/A1-101.
66. W.D.Apel et al. Conference paper No. 1164/A1-67.
67. O.I.Dahl et al. Conference paper No. 968/A1-129.
68. V.K.Birulev et al. Conference paper No. 18/A1-18.
69. K.F.Albrecht et al. Conference paper No. 12/A1-12.
70. V.I.Lisin et al. Nucl.Phys., B40, 298 (1972).

71. A.Babaev et al. CERN Preprint (1975).
72. H.R.Barton et al. Conference paper No. 1234/A1-165.
73. V.N.Bolotov et al. EPS International Conference on High Energy Physics, rep. L-61 Palermo (1975).
74. V.V.Isakov et al. Conference paper No. 39/A1-39.
75. K.G.Boreskov, S.T.Sukhorukov, K.A.Ter-Martirosyan. Yad.Fiz., 21, 825 (1975).
76. A.Bouqet et al. Conference papers No. 797/A1-88, 798/A1-89.
77. E.Leader. Phys.Lett., 60B, 290 (1976).
78. J.N.Carney et al. Conference paper No. 62/A1-62.
79. D.C.Colley et al. Conference paper No. 881/A1-137.
80. G.W.Brandenburg et al. Conference paper No. 288/A1-105.
81. G.W.Brandenburg et al. Conference paper No. 282/A1-119, and Phys.Lett., 59B, 405 (1975).
P.Estabrooks et al. Phys.Lett., 60B, 473 (1976); SLAC PUB 1730.
82. B.Chaurand et al. Conference paper No. 70/A1-70.
83. M.Aguilar-Benitez et al. Conference paper No. 294/A1-87.
84. Amsterdam-CERN-Nijmegen-Oxford Collab. Conf. paper No. 300/A1-133.
85. - " - No. 293/A1-140.
86. - " - No. 298/A1-141.
87. - " - No. 301/A1-127.
88. M.H.Shaevitz et al. Phys.Rev.Lett., 36, 8 (1976) and Conference paper No. 404/A1-100.
89. R.Honecker et al. Conference paper No. 48/A1-48.
90. H.Grässler et al. Conference paper No. 49/A1-49.
91. Aachen-Berlin-Bonn-CERN Coll.Conference paper No. 51/A1-51.
92. M.W.Arenton et al. Conference paper No. 794/A1-112.
93. N.Kwak et al. Conference paper No. 76/A1-76.
94. H.Becker et al. Conference paper No. 795/A1-132.
95. V.N.Bolotov et al. Conference paper No. 44/A1-44.
96. K.G.Boreskov, A.B.Kaidalov, L.A.Ponomarev. Preprint ITEP-950 (1972).
97. P.Estabrooks, A.D.Martin. Phys.Lett., 42B, 229 (1972).
98. A.C.Irving. Nucl.Phys., B105, 491 (1976).
99. N.N.Achasov et al. Conference paper No. 4/A1-4.
100. G.Goggi. CERN Preprint (1975).
M.Derrick. ANL-HEP-CP-75-52.
D.W.G.S.Leith. SLAC-PUB-1646 (1975).
H.I.Miettinen. Preprint CERN TH.2072 (1975).
A.B.Kaidalov, V.A.Khoze. Preprint LIYF-193 (1975).
101. H. de Kerret et al. Conference paper No. 65/A1-65.
102. A.I.Babaev et al. Conference paper No. 29/A1-29.
103. J.Biel et al. Conference papers No. 909/A1-8, 69/A1-69.
104. CERN-Pavia-Zurich Collab., Conference paper No. 338/A1-102.
105. V.Bakken et al. Conference paper No. 74/A1-74.
106. Aachen-Berlin-Bonn-CERN Collab. Conference paper No. 52/A1-52.
107. J.Ballam et al. Conference paper No. 1260/A1-143.
108. V.Kistiakowsky et al. Conference paper No. 742/A1-113.
109. Aachen-Berlin-Bonn-CERN-Cracow-Heidelberg Collab., Conference paper No. 1156/A1-157.
110. M.Della Negra et al. Conference paper No. 128/A1-85.
111. H. de Kerret et al. Conference paper No. 77/A1-77.
112. France-Soviet Union and CERN-Soviet Union Collab. Conference paper No. 1036/A1-142.
113. Saclay-Ecole Polytechnique-Rutherford Collab. Conference papers No. 72/A1-72, 73/A1-73.
114. R.K.Carnegie et al. Conference paper No. 287/A1-117.
115. Brussels - CERN - Mons - Serpukhov Collab. Conference paper No. 46/A1-46.
116. France-Soviet Union and CERN-Soviet Union Collab. Conference papers No. 38/A1-38, 1165/A1-121.
117. Yu. Kamyshkov. Talk at this Conference.
118. L.A.Ponomarev. Talk at this Conference and Conference paper No. 32/A1-32, 34/A1-34, 1038/A1-94.
119. F.Hayot et al. Conference paper No. 1211/A1-164.
120. M.Uehara. Conference paper No. 68/A1-68.
121. A.Minaka et al. Conference paper No. 371/A1-86.
122. T.Hirose et al. Conference paper No. 406/A1-110.
123. H.R.Gerhold, W.Majerotto. Conference paper No. 393/A1-111.
124. M.G.Albrow et al. Nucl.Phys., B72, 376 (1976) and Conference paper No. 799/A1-90.
125. Yu.Akimov et al. Phys.Rev.Lett., 35, 763 (1975) and talk by S.V.Mukhin at this Conference.
126. J.C.M.Armitage et al. Conference paper No. 345/A2-74.

127. R.D.Schamberger et al. Phys.Rev.Lett., 34, 1121 (1975); and preprint
128. J.M.Chapman et al. Phys.Rev.Lett., 32, 257 (1974).
129. S.J.Barish et al. Phys.Rev.Lett., 31, 1080 (1973).
130. F.T.Dao et al. Phys.Lett., 45B, 399 (1973).
131. ACGHT Collab., Nucl.Phys., B79, 1 (1974).
132. Rutgers-Imperial College Collab. Phys.Rev. Lett., 31, 1527, 1530 (1973).
133. M.G.Albrow et al. Nucl.Phys., B102, 275 (1976).
134. R.Webb et al. Phys.Lett., 55B, 331, 336 (1975).
135. W.Lockman et al. Conference paper No. 1210/A1-163.
136. A.B.Kaidalov et al. JETP Letters, 17, 626 (1973); Phys.Lett., B45, 493 (1973).
137. A.Capella. Phys.Rev., D8, 2047 (1973).
138. D.P.Roy, R.G.Roberts. Nucl.Phys., 77B, 240 (1974).
139. R.D.Field, G.C.Fox. Nucl.Phys., B80, 367 (1974).
140. A.B.Kaidalov, K.A.Ter-Martirosyan. Nucl. Phys., B75, 471 (1974).
141. Yu.M.Kazarinov et al. JINR, E2-9218, Dubna (1975) and Conference paper No. 1015/A1-151.
142. T.Inami, R.G.Roberts. RL-75-025.
143. L.Baksay et al. Phys.Lett., 53B, 484; 55B, 491 (1975).
144. M.Cavalli-Sforza et al. Nuovo Cimento Lett., 14, 345, 353, 359 (1975).
145. A.B.Kaidalov. Theoretical Introduction to Double Pomeron Exchange. In the Summary of the 18th ISR Discussion Meeting between Experimentalists and Theorists. CERN/TH.
146. L.Baksay et al. Phys.Lett., 61B, 89 (1976).
147. D.Denegri et al. Nucl.Phys., B98, 189 (1975).
148. M.Derrick et al. Phys.Rev.Lett., 32, 80 (1974).
149. B.Musgrave. ANL-HEP-CP-75-31.
150. L.A.Didenko et al. Conference paper No. 6/A1-6.